

Top-quark pair production via polarized and unpolarized protons in the supersymmetric QCD ^{*}

Yu Zeng-Hui ^{a,c} H. Pietschmann ^a Ma Wen-Gan ^{b,c} Han Liang ^c Jiang Yi ^c

^aInstitut für Theoretische Physik, Universität Wien, A-1090 Vienna, Austria

^bCCAST (World Laboratory), P.O.Box 8730, Beijing 100080, P.R.China

^cDepartment of Modern Physics, University of Science and Technology of China (USTC), Hefei, Anhui 230027, P.R.China

ABSTRACT

The QCD corrections to the top-quark pair production via both polarized and unpolarized gluon fusion in pp collisions are calculated in the Minimal Supersymmetric Model(MSSM). We find MSSM QCD corrections can reach 4% and may be observable in future precise experiments. Furthermore, we studied CP violation in MSSM, the results show that the CP violating parameter is sensitive to the masses of SUSY particles (It becomes zero, when the c.m. energy is less than twice the masses of both gluino and stop quarks.) and may reach 10^{-3} .

PACS number(s): 13.65.+i, 13.88.+e, 14.65.-q, 14.80.Dq, 14.80.Gt

^{*}Supported in part by Committe of National Natural Science Foundation of China and Project IV.B.12 of scientific and technoligical cooperation agreement between China and Austria

I. Introduction

The minimal supersymmetric model (MSSM) [1] is one of the most interesting extensions of the Standard Model (SM). Therefore testing the MSSM has attracted much interest. As is well known, MSSM predicts supersymmetric (SUSY) partners to each particle expected by SM, and searching for their existence is very important.

Since the top-quark was already found experimentally by the CDF and D0 Collaborations at Fermilab [2], we believe that more and more experimental events including top-quark will be collected in future experiments. That gives us a good chance to study the physics in top-quark pair production from pp or $p\bar{p}$ collisions with more precise experimental results. Because of the heavy mass of the top quark this process provides a test of the SM and possible signals of new physics at high energy.

The dominant subprocesses of top-quark pair production in pp or $p\bar{p}$ colliders are quark-antiquark annihilation and gluon-gluon fusion. The lowest order of those two subprocesses has been studied in Ref. [3]. There it was found that the former subprocess ($q\bar{q}$ annihilation) is more dominant in $p\bar{p}$ collisions when the c.m. energy(\sqrt{s}) is near the threshold value $2m_t$, whereas subprocess via gg fusion will get more and more important with increasing c.m. energy, and can become the most dominant one when the c.m. energy is much larger than $2m_t$.

In Ref. [4], QCD corrections to top-quark pair production in $p\bar{p}$ collisions have been studied in the frame of SM. It may seem natural that QCD corrections of those processes in the frame of MSSM are important for distinguishing those two models. Recently, the

SUSY QCD corrections to top pair production via $q\bar{q}$ annihilation were given in Ref. [5]. The SUSY QCD corrections via unpolarized gluon-gluon fusion were presented by C.S.Li. et. al [6].

It is obvious that the correction from SUSY QCD is related to the masses of top-quark and SUSY particles. Assuming the SUSY breaking scale at about 1 TeV, masses of SUSY particles would be smaller than 1 TeV. So we can hope that corrections from SUSY particles are significant since the heavy mass of the top quark ($m_t = 175.6 \pm 5.5$ GeV (world average)) may be comparable to some of the light SUSY particle masses. Therefore the SUSY QCD correction would give us some significant indirect information about the existence of SUSY particles.

Recently, the spin structure of the nucleon has been intensely studied by polarized deep inelastic scattering experiments at CERN and SLAC. This knowledge allows us to find a clear signal beyond the SM, if we collect enough events in the process of top-quark pair production from polarized pp or $p\bar{p}$ collisions. In SM QCD, there is no CP violation mechanism, whereas in SUSY QCD, the situation may be different. If we introduce phase angles of gluon partner and quark partners, we can get CP violation in MSSM QCD [7]. Once we get enough statistics of top-quark pairs from pp or $p\bar{p}$ colliders at higher energy, it will be possible to test CP violation. On the other hand, the spin-dependent parton distributions can be obtained from their polarized structure function data in Ref. [8]. There one found that the shape of polarized gluon and quark distributions in the nucleon depends on its polarization. Therefore the CP violation effects through the process of

top-quark pair production via gg fusion may be observed in polarized pp or $p\bar{p}$ collisions.

In this work we concentrate on the SUSY QCD corrections to the process $pp \rightarrow gg \rightarrow t\bar{t}X$ both in polarized and unpolarized colliding beams. In section 2, we give the tree level contribution to subprocess $gg \rightarrow t\bar{t}$. In section 3 we give the analytical expressions of SUSY QCD corrections to $gg \rightarrow t\bar{t}$. In section 4 the numerical results of the subprocess $gg \rightarrow t\bar{t}$ and the process $pp \rightarrow gg \rightarrow t\bar{t}X$ are presented. The conclusion is given in section 5. Some details of the expressions are listed in the appendix.

II. The Tree-Level Subprocess

The graphical representation of the process $g(\lambda_1, k_1)g(\lambda_2, k_2) \rightarrow t(p_1)\bar{t}(p_2)$ is shown in Fig.1 (a). The Mandelstam variables are defined as usual

$$\hat{s} = (p_1 + p_2)^2 = (k_1 + k_2)^2 \quad (2.1)$$

$$\hat{t} = (p_1 - k_1)^2 = (k_2 - p_2)^2 \quad (2.2)$$

$$\hat{u} = (p_1 - k_2)^2 = (k_1 - p_2)^2 \quad (2.3)$$

so $\hat{s} + \hat{t} + \hat{u} = 2m_t^2$. The amplitude of tree-level diagrams with polarized gluons can be written as:[3]

$$M_0^{(l)} = g_s^2 \epsilon^{\mu,a}(\lambda_1, k_1) \epsilon^{\nu,b}(\lambda_2, k_2) \bar{u}_i(p_1) T_{\mu\nu}^{ab(l)} v_j(p_2), \quad (l = s, t, u) \quad (2.4)$$

with

$$T_{\mu\nu}^{ab(s)} = \frac{T_{ij}^c f_{abc}}{s} [(\not{k}_1 - \not{k}_2) g_{\mu\nu} + (2k_2 + k_1)_\mu \gamma_\nu - (2k_1 + k_2)_\nu \gamma_\mu] \quad (2.5)$$

$$T_{\mu\nu}^{ab(t)} = \frac{-iT_{im}^a T_{mj}^b}{t-m_t^2} \gamma_\mu (\not{k}_2 - \not{p}_2 + m_t) \gamma_\nu \quad (2.6)$$

$$T_{\mu\nu}^{ab(u)} = \frac{-iT_{im}^b T_{mj}^a}{u-m_t^2} \gamma_\nu (\not{k}_1 - \not{p}_2 + m_t) \gamma_\mu \quad (2.7)$$

We chose a form in which only physical polarizations of gluons remained:

$$\epsilon^{\mu*}(\lambda_1, k_i) \epsilon^\nu(\lambda_2, k_i) = \frac{\delta_{\lambda_1, \lambda_2}}{2} (-g^{\mu\nu} + \frac{n^\mu k_i^\nu + n^\nu k_i^\mu}{n \cdot k_i} - \frac{n^2 k_i^\mu k_i^\nu}{(n \cdot k_i)^2} + i \lambda_1 \epsilon^{\sigma\mu\rho\nu} \frac{k_{i\sigma} n_\rho}{n \cdot k_i}) \quad (2.8)$$

Where $n = k_1 + k_2$, $\lambda_{1,2} = \pm 1$. From that, we can get the cross section at the tree-level with both polarized and unpolarized gluons.

III. SUSY QCD corrections (non-SM) to the subprocess $gg \rightarrow t\bar{t}$

1. Relevant MSSM Lagrangian.

The difference between the MSSM QCD and the SM QCD corrections stems from the interactions of SUSY particles. Thus we can divide SUSY QCD corrections into a standard and a non-standard part. The Lagrangian density of the non-SM part of the SUSY QCD interaction is written as:

$$L = L_1 + L_2 + L_3 + L_4 \quad (3.a.1)$$

Where

$$L_1 = -ig_s A_\mu^a T_{jk}^a (\tilde{q}_{jL} \partial_\mu \tilde{q}_{kL} - \tilde{q}_{kL} \partial_\mu \tilde{q}_{jL}) + (L \rightarrow R) \quad (3.a.2)$$

$$L_2 = -\sqrt{2} g_s T_{jk}^a (\bar{g}^a P_L q_k \tilde{q}_{jL}^* + \bar{q}_j P_R g^a \tilde{q}_{kL} - \bar{g}^a P_R q_k \tilde{q}_{jR}^* - \bar{q}_j P_L g^a \tilde{q}_{kR}) \quad (3.a.3)$$

$$L_3 = \frac{i}{2} g_s f_{abc} \bar{g}^a \gamma_\mu \tilde{g}^b A_\mu^c \quad (3.a.4)$$

$$L_4 = \frac{1}{6} g_s^2 A_\mu^a A^{\mu a} (\tilde{q}_L^* \tilde{q}_L + \tilde{q}_R^* \tilde{q}_R) + \frac{1}{2} g_s^2 d_{abc} A_\mu^a A^{\mu b} (\tilde{q}_{iL}^* T_{ij}^c \tilde{q}_{jL} + \tilde{q}_{iR}^* T_{ij}^c \tilde{q}_{jR}) \quad (3.a.5)$$

q stands for top-quark, \tilde{q} for stop-quark, \tilde{g} for gluino, P_L and P_R for left, right helicity projections, respectively. Here we only considered the SUSY QCD effect from stop-quark, because we assume that other scalar SUSY quarks are much heavier than the stop-quark and hence decoupled. Furthermore we introduce the phase ϕ_A and $\phi_{\tilde{g}}$ in the stop mixing matrix and a Majorana mass term for the gluino [7]. Defining θ as stop mixing angle, we get

$$\tilde{q}_L = e^{\frac{-i\phi}{2}} (\cos\theta \tilde{q}_1 + \sin\theta \tilde{q}_2) \quad (3.a.6)$$

$$\tilde{q}_R = e^{\frac{i\phi}{2}} (-\sin\theta \tilde{q}_1 + \cos\theta \tilde{q}_2) \quad (3.a.7)$$

where we define $\phi = \phi_A - \phi_{\tilde{g}}$ and suppose $m_{\tilde{q}_1} \leq m_{\tilde{q}_2}$.

2. Analytical results of the MSSM QCD corrections.

The one-loop SUSY QCD corrections are shown in Fig.1 (b). In the following we give only the contributions of s-channel and t-channel, the amplitude of u-channel can be obtained from the t-channel by exchanging: $t \leftrightarrow u$, $k_1 \leftrightarrow k_2$, $\epsilon_\mu^a(k_1) \leftrightarrow \epsilon_\nu^b(k_2)$, $T^a \leftrightarrow T^b$. We divided one-loop diagrams into three groups: Fig.1 (b.1) for self-energy diagrams of gluon and top-quark, Fig.1 (b.2) for vertex diagrams of gtt and ggg , Fig.1 (b.3) for box diagrams. The ultraviolet divergence are treated by dimensional regularization. We take the following renormalization scheme [9]: for coupling-constant renormalization we choose the modified Minimal Subtraction (\bar{MS}) scheme at charge-renormalization scale μ_R . The heavy particles (gluino, stop-quarks, etc.) are removed from the μ_R evolution of $\alpha_S(\mu_R^2)$, then they are decoupled smoothly when momenta are smaller than their masses. We define masses of heavy particles as pole masses.

The amplitude including all non-Standard SUSY QCD one-loop corrections can be written as:

$$\delta M = \delta M_s + \delta M_v + \delta M_{box} + \delta M_d. \quad (3.b.1)$$

The amplitude of self-energy diagrams δM_s (Fig.1.(b.1)) can be decomposed into δM_s^g (gluon self-energy) and δM_s^q (top-quark self-energy), i.e.

$$\begin{aligned} \delta M_s &= \delta M_s^g + \delta M_s^q \\ &= \delta M_s^{g(s)} + \delta M_s^{g(t)} + \delta M_s^{g(u)} + \delta M_s^{q(t)} + \delta M_s^{q(u)}. \end{aligned} \quad (3.b.2)$$

The amplitudes $\delta M_s^{g(s)}$, $\delta M_s^{g(t)}$ and $\delta M_s^{g(u)}$ for s-, t- and u-channel respectively can be expressed as:

$$\delta M_s^{g(s)} = \frac{1}{2} M_0^{(s)} [\Pi(k_1^2) + \Pi(k_2^2) + 2\Pi(s)], \quad (3.b.3)$$

$$\delta M_s^{g(t)} = \frac{1}{2} M_0^{(t)} [\Pi(k_1^2) + \Pi(k_2^2)], \quad (3.b.4)$$

$$\delta M_s^{g(u)} = \frac{1}{2} M_0^{(u)} [\Pi(k_1^2) + \Pi(k_2^2)], \quad (3.b.5)$$

where

$$\begin{aligned} \Pi(k^2) &= -\frac{\alpha_S}{4\pi} (T_F(\bar{B}_0 + 4\bar{B}_1 + 4\bar{B}_{21})[k, m_{\tilde{t}_1}, m_{\tilde{t}_1}] + \\ &\quad T_F(\bar{B}_0 + 4\bar{B}_1 + 4\bar{B}_{21})[k, m_{\tilde{t}_2}, m_{\tilde{t}_2}] - 4C_A(\bar{B}_1 + \bar{B}_{21})[k, m_{\tilde{g}}, m_{\tilde{g}}] - \frac{1}{3}C_A). \end{aligned} \quad (3.b.6)$$

Where $C_F = \frac{4}{3}$, $T_F = \frac{1}{2}$, $C_A = 3$, $\bar{B}_0 = B_0 - \Delta$, $\bar{B}_1 = B_1 + \frac{1}{2}\Delta$ and $\bar{B}_{21} = B_{21} - \frac{1}{3}\Delta$.

with $\Delta = \frac{2}{\epsilon} - \gamma + \log(4\pi)$, $\epsilon = 4 - n$, and

$$\delta M_s^{q(t)} = g_s^2 \epsilon^{\mu,a}(k_1) \epsilon^{\nu,b}(k_2) \bar{u}_i(p_1) \Sigma_{\mu\nu,ij}^{ab(t)} v_j(p_2), \quad (3.b.7)$$

and

$$\Sigma_{\mu\nu,ij}^{ab(t)} = \frac{-iT_{ik}^a T_{lj}^b}{(t-m_t^2)^2} \gamma_\mu(\not{k}_2 - \not{p}_2 + m_t) \Sigma_{kl}(k_2 - p_2)(\not{k}_2 - \not{p}_2 + m_t) \gamma_\nu \quad (3.b.8)$$

with

$$\Sigma_{kl}(p) = C_F \frac{\alpha_S}{2\pi} (C_L \not{p} P_L + C_R \not{p} P_R - C_L^S P_L - C_R^S P_R) \delta_{kl} \quad (3.b.9)$$

$$C_L = x_1 x_3 B_1[p, m_{\tilde{g}}, m_{\tilde{t}_1}] + C_L^t + (m_{\tilde{t}_1} \rightarrow m_{\tilde{t}_2}, x_i \rightarrow y_i), \quad (3.b.10)$$

$$\begin{aligned} C_L^t &= \frac{1}{2}(\delta Z_L + \delta Z_L^\dagger) \\ &= -(x_1 x_3 \text{Re}[B_1] + m_t^2 (x_1 x_3 + x_2 x_4) \text{Re}[B'_1] - m_t m_{\tilde{g}} (x_2 x_3 + x_1 x_4) \text{Re}[B'_0]) [p, m_{\tilde{g}}, m_{\tilde{t}_1}]|_{p^2=m_t^2}, \end{aligned} \quad (3.b.11)$$

$$C_R = x_2 x_4 B_1[p, m_{\tilde{g}}, m_{\tilde{t}_1}] + C_R^t + (m_{\tilde{t}_1} \rightarrow m_{\tilde{t}_2}, x_i \rightarrow y_i), \quad (3.b.12)$$

$$\begin{aligned} C_R^t &= \frac{1}{2}(\delta Z_R + \delta Z_R^\dagger) \\ &= -(x_2 x_4 \text{Re}[B_1] + m_t^2 (x_1 x_3 + x_2 x_4) \text{Re}[B'_1] - m_t m_{\tilde{g}} (x_2 x_3 + x_1 x_4) \text{Re}[B'_0]) [p, m_{\tilde{g}}, m_{\tilde{t}_1}]|_{p^2=m_t^2}, \end{aligned} \quad (3.b.13)$$

$$C_L^S = x_2 x_3 m_{\tilde{g}} B_0[p, m_{\tilde{g}}, m_{\tilde{t}_1}] + C_L^{St} + (m_{\tilde{t}_1} \rightarrow m_{\tilde{t}_2}, x_i \rightarrow y_i), \quad (3.b.14)$$

$$\begin{aligned} C_L^{St} &= \frac{1}{2}(\delta Z_L + \delta Z_R^\dagger) + \delta m_t \\ &= -(x_2 x_3 m_{\tilde{g}} \text{Re}[B_0] + m_t^3 (x_1 x_3 + x_2 x_4) \text{Re}[B'_1] - 2m_t^2 m_{\tilde{g}} x_2 x_3 \text{Re}[B'_0]) [p, m_{\tilde{g}}, m_{\tilde{t}_1}]|_{p^2=m_t^2}, \end{aligned} \quad (3.b.15)$$

$$C_R^S = x_1 x_4 m_{\tilde{g}} B_0[p, m_{\tilde{g}}, m_{\tilde{t}_1}] + C_R^{St} + (m_{\tilde{t}_1} \rightarrow m_{\tilde{t}_2}, x_i \rightarrow y_i), \quad (3.b.16)$$

$$\begin{aligned} C_R^{St} &= \frac{1}{2}(\delta Z_R + \delta Z_L^\dagger) + \delta m_t \\ &= -(x_1 x_4 m_{\tilde{g}} \text{Re}[B_0] + m_t^3 (x_1 x_3 + x_2 x_4) \text{Re}[B'_1] - 2m_t^2 m_{\tilde{g}} x_1 x_4 \text{Re}[B'_0]) [p, m_{\tilde{g}}, m_{\tilde{t}_1}]|_{p^2=m_t^2}, \end{aligned} \quad (3.b.17)$$

We use the following abbreviations: $x_1 = \cos \theta e^{-i\phi}$, $x_2 = \sin \theta e^{i\phi}$, $x_3 = \cos \theta e^{i\phi}$, $x_4 = \sin \theta e^{-i\phi}$, $y_1 = \sin \theta e^{-i\phi}$, $y_2 = -\cos \theta e^{i\phi}$, $y_3 = \sin \theta e^{i\phi}$ and $y_4 = -\cos \theta e^{-i\phi}$.

The amplitude of vertex diagrams can be expressed as:

$$\delta M_v^{(l)} = g_s \epsilon^{\mu, a}(k_1) \epsilon^{\nu, b}(k_2) \bar{u}_i(p_1) \Lambda_{\mu\nu, ij}^{ab(l)} v_j(p_2), \quad (l = s, t, u), \quad (3.b.18)$$

where

$$\begin{aligned} \Lambda_{\mu\nu}^{ab(s)} = & -\frac{T_{ij}^c}{s} \Lambda_{\mu\nu\rho}^g(k_1, k_2, k_1 + k_2) \gamma_\rho \\ & -\frac{f_{abc}}{s} [(k_1 - k_2)_\rho g_{\mu\nu} + (2k_2 + k_1)_\mu g_{\nu\rho} \\ & \quad - (2k_1 + k_2)_\nu g_{\mu\rho}] \Lambda_{\rho,ij}^{c(t)}(k_1 + k_2, p_1, p_2) \end{aligned} \quad (3.b.19)$$

and

$$\begin{aligned} \Lambda_{\mu\nu}^{ab(t)} = & \frac{-i}{t - m_t^2} [T_{mj}^b \Lambda_{\mu,im}^{a(t)}(k_1, p_1, k_1 - p_1) (\not{k}_2 - \not{p}_2 + m_t) \gamma_\nu \\ & + T_{im}^a \gamma_\mu (\not{k}_2 - \not{p}_2 + m_t) \Lambda_{\nu,mj}^{b(t)}(k_2, k_2 - p_2, p_2)]. \end{aligned} \quad (3.b.20)$$

The functions $\Lambda_{\mu\nu,ij}^{ab(l)}$ are listed in the Appendix.

The box diagram corrections (Fig.1(b.3)) are given as follows:

$$\begin{aligned} \delta M_{box}^{(t)} = & 2g_s^2 \epsilon^{\mu,a}(k_1) \epsilon^{\nu,b}(k_2) \bar{u}_i(p_1) ((T^c T^a T^b T^c)_{ij} F^{(t\alpha)} \\ & - i f_{bcd} (T^c T^a T^d)_{ij} F^{(t\beta)} - f_{acm} f_{bmd} (T^c T^d)_{ij} F^{(t\gamma)} \\ & - [T^c (T^a T^b + T^b T^a) T^c]_{ij} F^{(t\delta)}) v_j(p_2), \end{aligned} \quad (3.b.21)$$

The factors $F^{(ti)}(i = \alpha, \beta, \gamma, \delta)$ correspond to the four Feynman diagrams in Fig.1(b.3)

respectively and are given explicitly in the Appendix. The decoupling part is:

$$\delta M_d = M_0 \left(\frac{\alpha_S(\mu)}{\pi} \right) \left[\frac{1}{48} \log \left(\frac{\mu_R^2}{m_{\tilde{t}_1}^2} \right) + \frac{1}{48} \log \left(\frac{\mu_R^2}{m_{\tilde{t}_2}^2} \right) + \frac{1}{4} \log \left(\frac{\mu_R^2}{m_{\tilde{g}}^2} \right) \right] \quad (3.b.22)$$

Now we can get the total cross section:

$$\begin{aligned} \sigma(\lambda_1, \lambda_2) &= \sigma_0(\lambda_1, \lambda_2) (1 + \delta\sigma(\lambda_1, \lambda_2)) \\ &= \frac{1}{16\pi s^2} \int_{t^-}^{t^+} dt \sum_{spins} [|M_0|^2 + 2\text{Re}(M_0^\dagger \delta M)] \end{aligned} \quad (3.b.23)$$

where $t^\pm = (m_t^2 - \frac{1}{2}s) \pm \frac{1}{2}s\beta_t$, $\beta_t = \sqrt{1 - 4m_t^2/s}$, and the spin sum is performed only over the final quark pair when we considered polarized gluons. For unpolarized results, average over initial spins.

IV. Numerical results

We write $\hat{\sigma}_0$ for the Born cross section and $\hat{\sigma}$ for the cross section including one-loop SUSY QCD corrections of subprocess $gg \rightarrow t\bar{t}$, and define $\hat{\delta} = \frac{\hat{\sigma} - \hat{\sigma}_0}{\hat{\sigma}_0}$. For polarized

gluon fusions, $\hat{\sigma}_{++}$, $\hat{\sigma}_{--}$ and $\hat{\sigma}_{+-}$ are the cross sections with positive, negative and mixed polarization of the gluons. In order to inspect the CP violating effects we introduce the CP-violation parameter defined by $\xi_{CP} = \frac{\hat{\sigma}_{++} - \hat{\sigma}_{--}}{\hat{\sigma}_{++} + \hat{\sigma}_{--}}$.

The observable SUSY QCD effects in $gg \rightarrow t\bar{t}$ should be found in pp colliders. The SUSY QCD contribution to the process $p(P_1, x)p(P_2, y) \rightarrow gg \rightarrow t\bar{t}X$ (x,y are polarizations of protons) can be obtained by convoluting the subprocess with gluon distribution functions.

$$\sigma(s) = \int dx_1 dx_2 G(x_1, Q) G(x_2, Q) \hat{\sigma}(\hat{s}, \alpha_s(\mu)) \quad (4.1)$$

with $k_1 = x_1 P_1$, $\tau = x_1 x_2 = \hat{s}/s$. $G(x_i, Q)$ ($i = 1, 2$) are gluon distribution functions of protons. We take $Q = \mu_R = 2m_t$.

In order to get results of top quark pair production from polarized pp collisions, we need to consider the polarized gluon distributions in protons. The cross sections of polarized $pp \rightarrow gg \rightarrow t\bar{t}X$ can be written as

$$\sigma(x, y) = \sum_{\lambda_1, \lambda_2 = \pm} \int dx_1 dx_2 G^{x\lambda_1}(x_1, Q) G^{y\lambda_2}(x_2, Q) \hat{\sigma}_{\lambda_1, \lambda_2}(\hat{s}, \alpha_s(\mu)) \quad (4.2)$$

where x and y are the polarizations of incoming protons and λ_1 , λ_2 are the polarizations of gluons inside protons. $G^{x\lambda_1}(x, Q)$, $G^{y\lambda_2}(x, Q) = G^{\pm}(x, Q)$ for equal (+) and opposite (-) polarization, $G^+(x, Q)$ and $G^-(x, Q)$ are polarized gluon distribution functions in the proton. We used the polarized proton structure functions $G^+(x, Q)$ and $G^-(x, Q)$ of Brodsky et al. [8] in our numerical calculations.

The SUSY QCD corrections of the process $pp \rightarrow gg \rightarrow t\bar{t}X$ are shown in Fig.2 (a) and

ξ_{CP} versus c.m. energy \sqrt{s} in Fig.2 (b). The SUSY QCD corrections are about $2\% \sim 4\%$ and decrease with increasing c.m. energy. Thus they are within reach of future precision experiments and provide a possible discrimination of SM and MSSM effects. From Fig.2(b) we can see that the CP violation parameter ξ_{CP} can be 10^{-3} when c.m. energy is about 1 TeV. Therefore, even CP violation stemming from SUSY QCD can in principle be tested in future precision experiments. That would help us to learn more about the sources of CP violation.

In order to explore the effects of SUSY correction for future arrangements of optimal experimental conditions we also give details of the subprocess $gg \rightarrow t\bar{t}$.

SUSY QCD corrections versus c.m. energy ($\sqrt{\hat{s}}$) for different polarization gluons are plotted in Fig.3(a \sim c) ($m_{\tilde{g}} = 200$ GeV, $m_{\tilde{t}_1} = 250$ GeV, $m_{\tilde{t}_2} = 450$ GeV, and $\theta = \phi = 45^\circ$). In Fig.3(a) $\delta\hat{\sigma}_{++}$ and $\delta\hat{\sigma}_{--}$ are drawn with solid line and dashed line, respectively. $\delta\hat{\sigma}_{+-}$ is depicted in Fig.3 (c) and ξ_{CP} as a function of c.m. energy is shown in Fig.3(b). The results show that $\delta\hat{\sigma}_{++}$ and $\delta\hat{\sigma}_{--}$ approach equal values when the c.m. energy is far beyond its threshold value $2m_t$, but the quantitative difference between $\delta\hat{\sigma}_{+-}$ and $\delta\hat{\sigma}_{++}$ still exists in all energy ranges. We find that ξ_{CP} will be zero if the c.m. energy is below the threshold of SUSY particles in the loop. ξ_{CP} has the obvious threshold effect at points $\sqrt{\hat{s}} = 2m_{\tilde{g}}$ or $2m_{\tilde{t}_i}$, ($i = 1, 2$). This is reasonable because only beyond those points can we have absorptive terms which give contributions to ξ_{CP} . We also found that the two stop quarks give opposite contributions to ξ_{CP} so when their masses are degenerate ξ_{CP} will vanish. (See Fig.5, 6) With increasing c.m. energy, ξ_{CP} will drop because the

contributions from two stop quarks will cancel each other. So a strong change of ξ_{CP} with c.m. energy can be an indication of effects of stop quarks and gluino.

$\hat{\sigma}(\pm, \pm)$ and ξ_{CP} as function of $m_{\tilde{g}}$ are shown in Fig.4 (a) and Fig.4 (b), respectively ($\sqrt{\hat{s}} = 500GeV$, $m_{\tilde{t}_1} = 100GeV$, $m_{\tilde{t}_2} = 450GeV$, $\theta = \phi = 45^\circ$). We can see that ξ_{CP} changes its sign when $m_{\tilde{g}}$ is near m_t , and again has threshold effects when $\sqrt{\hat{s}} = 2 m_{\tilde{g}}$. There is a small peak around $m_{\tilde{g}} = 250GeV$ in Fig.3 (a) from a resonance effect at $\sqrt{\hat{s}} = 2m_{\tilde{g}}$.

Dependences of $\delta\hat{\sigma}(\pm, \pm)$ and ξ_{CP} on $m_{\tilde{t}_1}$ are plotted in Fig.5 (a) and Fig.5 (b). $\delta\hat{\sigma}(\pm, \pm)$ and ξ_{CP} as functions of $m_{\tilde{t}_2}$ are shown in Fig.6 (a) and Fig.6 (b), respectively. In all parts of Fig.5 and Fig.6, we take $\sqrt{\hat{s}} = 500GeV$, $m_{\tilde{g}} = 200GeV$ and $\theta = \phi = 45^\circ$. But in Fig.6, we set $m_{\tilde{t}_2} = 450GeV$ and in Fig.7, we have $m_{\tilde{t}_1} = 100GeV$. We found that ξ_{CP} in fact increases with mass splitting of stop-quarks (i.e. $m_{\tilde{t}_2} - m_{\tilde{t}_1}$), and when $m_{\tilde{t}_1} = m_{\tilde{t}_2}$, ξ_{CP} is equal to zero. Superimposed is the threshold effect of stop quark ($\sqrt{\hat{s}} = 2 m_{\tilde{t}_i}$). At those points we find a sharp change of ξ_{CP} . Again the resonance effect can be seen in Fig.5(a) and Fig.6(a) arround $m_{\tilde{t}_i} \sim \frac{\sqrt{\hat{s}}}{2} = 250 GeV$, ($i = 1, 2$).

Finally, dependence of $\delta\hat{\sigma}_{\pm\pm}$ and ξ_{CP} on the phase ϕ is shown in Fig.7 (a) and (b). We find that $\xi_{CP} \sim \sin(2\phi)$ and reaches its maximum value when $\phi = \frac{\pi}{4}$.

IV. Conclusion

In this work we have studied the one-loop supersymmetric QCD corrections of the process $gg \rightarrow t\bar{t}$ and its contribution to $pp \rightarrow gg \rightarrow t\bar{t}X$. The calculations show that SUSY QCD

effects are significant. The absolute values of the corrections are about $2\% \sim 4\%$, so they may be found in future precision experiments. Furthermore, we find ξ_{CP} depends strongly on masses of SUSY particles and can reach 10^{-3} when we take plausible SUSY parameters.

The results show that there is an obvious difference between the corrections for the protons polarized with parallel spin and that with anti-parallel spin. Hence there is a possibility to study spin-dependence in the frame of MSSM QCD.

We also give results of the subprocess $gg \rightarrow t\bar{t}$. We find that when the c.m. energy passes through the value $2m_{\tilde{g}}$ or $2m_{\tilde{t}_i}$ ($i = 1, 2$), ξ_{CP} changes strongly. If c.m. energy is less than $2m_{\tilde{g}}$ and $2m_{\tilde{t}_i}$ ($i = 1, 2$), ξ_{CP} will be zero. If a sharp change in ξ_{CP} is found from low c.m. energy to high c.m. energy in future experiments, it can be interpreted as a signal of SUSY. Furthermore, because the CP violating parameter ξ_{CP} depends strongly on the mass of gluino (as shown in Fig.4 (b)) and the mass splitting of stop-quarks $m_{\tilde{t}_2} - m_{\tilde{t}_1}$ (as shown in Fig.5 and Fig.6), we can also get these informations from measurements of ξ_{CP} .

This work was supported in part by the National Natural Science Foundation of China and the National Committee of Science and Technology of China. Part of this work was done when one of the authors, Ma Wen-Gan, visited the University Vienna under the scientific and technoligical cooperation agreement between China and Austria (project number: IV.B.12). The authors would like to thank Prof. A.Bartl for useful dissussions and comments.

Appendix

1. The vertex functions are given:

$$\Lambda_{\mu\nu\rho}^g(k_1, k_2, k_1 + k_2) = \frac{Ig_S^3}{16\pi^2} Tr(T^b T^c T^a) \Lambda_{1,\mu\nu\rho}^g - \frac{g_S^3}{16\pi^2} f^{cmn} f^{anl} f^{blm} \Lambda_{2,\mu\nu\rho}^g, \quad (A.1.1)$$

where the vertex function $\Lambda_{1,\mu\nu\rho}^g$ is written as

$$\begin{aligned} \Lambda_{1,\mu\nu\rho}^g = & f_{v1}^g g_{\mu\rho} k_{1\nu} + f_{v2}^g g_{\mu\nu} k_{1\rho} + f_{v3}^g g_{\nu\rho} k_{2\mu} + f_{v4}^g g_{\mu\nu} k_{2\rho} \\ & + f_{v5}^g k_{1\nu} k_{1\rho} k_{2\mu} + f_{v6}^g k_{1\nu} k_{2\rho} k_{2\mu} \\ & + (m_{\tilde{t}_1} \rightarrow m_{\tilde{t}_2}, x_i \rightarrow y_i), \end{aligned} \quad (A.1.2)$$

and

$$f_{v1}^g = -8\bar{C}_{24}^1 - 8\bar{C}_{35}^1, \quad (A.1.3)$$

$$f_{v2}^g = -4\bar{C}_{24}^1 - 8\bar{C}_{35}^1, \quad (A.1.4)$$

$$f_{v3}^g = -8\bar{C}_{36}^1, \quad (A.1.5)$$

$$f_{v4}^g = -4\bar{C}_{24}^1 - 8\bar{C}_{36}^1, \quad (A.1.6)$$

$$f_{v5}^g = 4C_{12}^1 + 12C_{23}^1 + 8C_{33}^1, \quad (A.1.7)$$

$$f_{v6}^g = 4C_{12}^1 + 8C_{22}^1 + 4C_{23}^1 + 8C_{34}^1, \quad (A.1.8)$$

Here we denote $C_{ij}^1 = C_{ij}[-k_1, -k_2, m_{\tilde{t}_1}, m_{\tilde{t}_1}, m_{\tilde{t}_1}]$. The another vertex function Λ_2^g can

be expressed as

$$\begin{aligned} \Lambda_{2,\mu\nu\rho}^g = & h_{v1}^g g_{\mu\rho} k_{1\nu} + h_{v2}^g g_{\mu\nu} k_{1\rho} + h_{v3}^g g_{\nu\rho} k_{2\mu} + h_{v4}^g g_{\mu\nu} k_{2\rho} \\ & + h_{v5}^g k_{1\nu} k_{1\rho} k_{2\mu} + h_{v6}^g k_{1\nu} k_{2\rho} k_{2\mu} \end{aligned} \quad (A.1.9)$$

with

$$h_{v1}^g = -8m_{\tilde{g}}^2 C_0^{(2)} - 4m_{\tilde{g}}^2 C_{11}^{(2)} - 16\bar{C}_{24}^{(2)} + 12\epsilon C_{24}^{(2)} - 8\bar{C}_{35}^{(2)} + 6\epsilon C_{35}^{(2)} + 8k_1 \cdot k_2 C_{12}^{(2)} + 16k_1 \cdot k_2 C_{23}^{(2)} + 8k_1 \cdot k_2 C_{33}^{(2)}, \quad (A.1.10)$$

$$h_{v2}^g = -4m_{\tilde{g}}^2 C_{11}^{(2)} - 8\bar{C}_{35}^{(2)} + 6\epsilon C_{35}^{(2)} + 8C_{23}^{(2)} k_1 \cdot k_2 + 8C_{33}^{(2)} k_1 \cdot k_2, \quad (A.1.11)$$

$$h_{v3}^g = 4m_{\tilde{g}}^2 C_0^{(2)} - 4m_{\tilde{g}}^2 C_{12}^{(2)} + 8\bar{C}_{24}^{(2)} - 6\epsilon C_{24}^{(2)} - 8\bar{C}_{36}^{(2)} + 6\epsilon C_{36}^{(2)} + 8k_1 \cdot k_2 C_{22}^{(2)} + 8k_1 \cdot k_2 C_{34}^{(2)}, \quad (A.1.12)$$

$$h_{v4}^g = -4m_{\tilde{g}}^2 C_0^{(2)} - 4m_{\tilde{g}}^2 C_{12}^{(2)} - 8\bar{C}_{24}^{(2)} + 6\epsilon C_{24}^{(2)} - 8\bar{C}_{36}^{(2)} + 6\epsilon C_{36}^{(2)} + 8k_1 \cdot k_2 C_{12}^{(2)} + 8k_1 \cdot k_2 C_{22}^{(2)} + 8k_1 \cdot k_2 C_{23}^{(2)} + 8k_1 \cdot k_2 C_{34}^{(2)}, \quad (A.1.13)$$

$$h_{v5}^g = -8C_{12}^{(2)} - 24C_{23}^{(2)} - 16C_{33}^{(2)} \quad (A.1.14)$$

$$h_{v6}^g = -8C_{12}^{(2)} - 16C_{22}^{(2)} - 8C_{23}^{(2)} - 16C_{34}^{(2)} \quad (A.1.15)$$

There $C_0^{(2)}, C_{ij}^{(2)} = C_0, C_{ij}[-k_1, -k_2, m_{\tilde{g}}, m_{\tilde{g}}, m_{\tilde{g}}]$ and $\bar{C}_{24}^{(2)} = C_{24}^{(2)} - \frac{1}{4}\Delta$, $\bar{C}_{35}^{(2)} = C_{35}^{(2)} + \frac{1}{6}\Delta$, $\bar{C}_{36}^{(2)} = C_{36}^{(2)} + \frac{1}{12}\Delta$.

The gtt vertex functions are shown as following:

$$\begin{aligned} \Lambda_{\mu,ij}^{a(t)}(k, p_1, p_2) = & -\frac{g_S^3}{16\pi^2}(2C_F - C_A)T_{ij}^a(\Lambda_{1L,\mu}^t + \Lambda_{1R,\mu}^t) \\ & -\frac{g_S^3}{16\pi^2}C_A T_{ij}^a(\Lambda_{2L,\mu}^t + \Lambda_{2R,\mu}^t) + \Lambda_{\mu ct}^t \\ & +(m_{\tilde{t}_1} \rightarrow m_{\tilde{t}_2}, x_i \rightarrow y_i). \end{aligned} \quad (A.1.16)$$

The expressions of $\Lambda_{1L,\mu}^t$, $\Lambda_{1R,\mu}^t$, $\Lambda_{2L,\mu}^t$ and $\Lambda_{2R,\mu}^t$ are given as following:

$$\begin{aligned} \Lambda_{1L,\mu}^t = & f_{v1L}^t \gamma_\mu + f_{v2L}^t p_{1\mu} + f_{v3L}^t \not{p}_1 p_{1\mu} + f_{v4L}^t \not{p}_2 p_{1\mu} \\ & + f_{v5L}^t p_{2\mu} + f_{v6L}^t \not{p}_1 p_{2\mu} + f_{v7L}^t \not{p}_2 p_{2\mu}, \end{aligned} \quad (A.1.17)$$

$$\Lambda_{1R,\mu}^t = \Lambda_{1L,\mu}^t(f_{vkL}^t \rightarrow f_{vkR}^t, (k = 1 \sim 7)). \quad (A.1.18)$$

where

$$f_{v1L}^t = -2x_2 x_4 C_{24}^{(3)} \quad (A.1.19)$$

$$f_{v2L}^t = x_2 x_3 m_{\tilde{g}} (C_0^{(3)} + 2C_{11}^{(3)}) \quad (A.1.20)$$

$$f_{v3L}^t = x_2 x_4 (C_0^{(3)} + 3C_{11}^{(3)} + 2C_{21}^{(3)}) \quad (A.1.21)$$

$$f_{v4L}^t = x_2 x_4 (C_{12}^{(3)} + 2C_{23}^{(3)}) \quad (A.1.22)$$

$$f_{v5L}^t = x_2 x_3 m_{\tilde{g}} (C_0^{(3)} + 2C_{12}^{(3)}) \quad (A.1.23)$$

$$f_{v6L}^t = x_2 x_4 (C_0^{(3)} + C_{11}^{(3)} + 2C_{12}^{(3)} + 2C_{23}^{(3)}) \quad (A.1.24)$$

$$f_{v7L}^t = x_2 x_4 (C_{12}^{(3)} + 2C_{22}^{(3)}) \quad (A.1.25)$$

there $C_0^{(3)}, C_{ij}^{(3)} = C_0, C_{ij}[-p_1, -p_2, m_{\tilde{t}_1}, m_{\tilde{g}}, m_{\tilde{t}_1}],$ and f_{vkR}^t can be obtained through exchanging $x_1 \leftrightarrow x_2$ and $x_3 \leftrightarrow x_4$ in f_{vkL}^t ($k=1,2,\dots,7$).

The function Λ_2^t is defined as:

$$\begin{aligned} \Lambda_{2L,\mu}^t = & h_{v1L}^t \gamma_\mu + h_{v2L}^t \gamma_\mu \not{p}_1 + h_{v3L}^t \gamma_\mu \not{p}_2 + h_{v4L}^t \not{p}_1 \gamma_\mu \\ & + h_{v5L}^t \not{p}_2 \gamma_\mu + h_{v6L}^t \not{p}_1 \gamma_\mu \not{p}_1 + h_{v7L}^t \not{p}_1 \gamma_\mu \not{p}_2 \\ & + h_{v8L}^t \not{p}_2 \gamma_\mu \not{p}_1 + h_{v9L}^t \not{p}_2 \gamma_\mu \not{p}_2 \end{aligned} \quad (A.1.26)$$

$$\Lambda_{2R,\mu}^t = \Lambda_{2L,\mu}^t (h_{vkL}^t \rightarrow h_{vkR}^t, (h = 1 \sim 9)). \quad (A.1.27)$$

$$h_{v1L}^t = x_2 x_4 (-m_{\tilde{g}}^2 C_0^{(4)} - 2C_{24}^{(4)} + \epsilon C_{24}^{(4)}) \quad (A.1.28)$$

$$h_{v2L}^t = x_2 x_3 m_{\tilde{g}}^2 (C_0^{(4)} + C_{11}^{(4)}) \quad (A.1.29)$$

$$h_{v3L}^t = x_2 x_3 m_{\tilde{g}}^2 (C_0^{(4)} + C_{12}^{(4)}) \quad (A.1.30)$$

$$h_{v4L}^t = x_2 x_3 m_{\tilde{g}}^2 C_{11}^{(4)} \quad (A.1.31)$$

$$h_{v5L}^t = x_2 x_3 m_{\tilde{g}}^2 C_{12}^{(4)} \quad (A.1.32)$$

$$h_{v6L}^t = -x_2 x_4 (C_{11}^{(4)} + C_{21}^{(4)}) \quad (A.1.33)$$

$$h_{v7L}^t = -x_2 x_4 (C_{11}^{(4)} + C_{23}^{(4)}) \quad (A.1.34)$$

$$h_{v8L}^t = -x_2 x_4 (C_{12}^{(4)} + C_{23}^{(4)}) \quad (A.1.35)$$

$$h_{v9L}^t = -x_2 x_4 (C_{12}^{(4)} + C_{22}^{(4)}) \quad (A.1.36)$$

where $C_0^{(4)}, C_{ij}^{(4)} = C_0, C_{ij}[-p_1, -p_2, m_{\tilde{g}}, m_{\tilde{t}_1}, m_{\tilde{g}}]$, and h_{vkR}^t can also be obtained by exchanging $x_1 \leftrightarrow x_2$ and $x_3 \leftrightarrow x_4$ in h_{vkL}^t .

The counter terms were given:

$$\Lambda_{\mu ct}^t = -C_F \frac{g_S^3}{8\pi^2} T_{ij}^a \gamma_\mu (C_L^t P_L + C_R^t P_R) \quad (A.1.37)$$

The expressions of C_L^t and C_R^t can be found in Eq.(3.b.11) and Eq.(3.b.13).

2. The form factors in Eq.(3.b.21) are expressed as following form:

$$\begin{aligned} F^{(ti)} = & \frac{i\alpha_S}{4\pi} P_L [\gamma_\mu \gamma_\nu f_{b1}^{(tiL)} + \gamma_\nu \gamma_\mu f_{b2}^{(tiL)} \\ & + p_{1\nu} \gamma_\mu f_{b3}^{(tiL)} + p_{2\nu} \gamma_\mu f_{b4}^{(tiL)} \\ & + p_{1\mu} \gamma_\nu f_{b5}^{(tiL)} + p_{2\mu} \gamma_\nu f_{b6}^{(tiL)} \\ & + \gamma_\mu \gamma_\nu \not{k}_1 f_{b7}^{(tiL)} + \gamma_\nu \gamma_\mu \not{k}_1 f_{b8}^{(tiL)} \\ & + \not{k}_1 p_{1\mu} p_{2\nu} f_{b9}^{(tiL)} + \not{k}_1 p_{2\mu} p_{1\nu} f_{b10}^{(tiL)} \\ & + \gamma_\mu \not{k}_1 p_{1\nu} f_{b11}^{(tiL)} + \gamma_\mu \not{k}_1 p_{2\nu} f_{b12}^{(tiL)} \\ & + \gamma_\nu \not{k}_1 p_{1\mu} f_{b13}^{(tiL)} + \gamma_\nu \not{k}_1 p_{2\mu} f_{b14}^{(tiL)} \\ & + p_{1\mu} p_{2\nu} f_{b15}^{(tiL)} + p_{1\mu} p_{1\nu} f_{b16}^{(tiL)} \\ & + p_{2\mu} p_{1\nu} f_{b17}^{(tiL)} + \not{k}_1 p_{1\mu} p_{1\nu} f_{b18}^{(tiL)} \\ & + \not{k}_1 p_{2\mu} p_{2\nu} f_{b19}^{(tiL)} + p_{2\mu} p_{2\nu} f_{b20}^{(tiL)}] \\ & + (P_L \rightarrow P_R, f_{bk}^{(tiL)} \rightarrow f_{bk}^{(tiR)}, (k = 1 \sim 20)) \end{aligned} \quad (A.2.1)$$

In Eq. (A.2.1), $i = \alpha, \beta, \gamma, \delta$. we only give the expressions of f_{bk}^{tiR} ($k = 1, 2, \dots, 20$) in Appendix. The expressions of f_{bk}^{tiL} can be obtained from f_{bk}^{tiR} by exchanging $x_1 \leftrightarrow x_2$ and $x_3 \leftrightarrow x_4$.

The expressions of f_{bk}^{tiR} can be expressed by the following parts. The expressions of

$f_{bk}^{t\alpha R}$ are given as below:

$$\begin{aligned} f_{b1}^{(t\alpha R)} &= f_{b2}^{(t\alpha R)} \\ &= -2x_1x_4m_{\tilde{g}}D_{27}^{(1)} + 2x_2x_4m_tD_{311}^{(1)} \\ &\quad + 2(x_1x_3 - x_2x_4)m_tD_{313}^{(1)}, \end{aligned} \quad (A.2.2)$$

$$f_{b3}^{(t\alpha R)} = 4x_1x_3(D_{311}^{(1)} - D_{312}^{(1)}), \quad (A.2.3)$$

$$f_{b4}^{(t\alpha R)} = -4x_1x_3(D_{27}^{(1)} + D_{312}^{(1)}), \quad (A.2.4)$$

$$f_{b5}^{(t\alpha R)} = 4x_1x_3(D_{27}^{(1)} + D_{311}^{(1)} - D_{313}^{(1)}), \quad (A.2.5)$$

$$f_{b6}^{(t\alpha R)} = -4x_1x_3D_{313}^{(1)}, \quad (A.2.6)$$

$$f_{b7}^{(t\alpha R)} = f_{b8}^{(t\alpha R)} = 2x_1x_3(D_{313}^{(1)} - D_{312}^{(1)}), \quad (A.2.7)$$

$$\begin{aligned} f_{b9}^{(t\alpha R)} &= 4x_1x_3(D_{13}^{(1)} - D_{12}^{(1)} - D_{22}^{(1)} - D_{23}^{(1)} - D_{24}^{(1)} \\ &\quad + D_{25}^{(1)} + 2D_{26}^{(1)} - D_{36}^{(1)} + D_{38}^{(1)} - D_{39}^{(1)} + D_{310}^{(1)}), \end{aligned} \quad (A.2.8)$$

$$f_{b10}^{(t\alpha R)} = 4x_1x_3(D_{37}^{(1)} - D_{39}^{(1)} + D_{38}^{(1)} - D_{310}^{(1)}), \quad (A.2.9)$$

$$f_{b11}^{(t\alpha R)} = f_{b12}^{(t\alpha R)} = f_{b13}^{(t\alpha R)} = f_{b14}^{(t\alpha R)} = 0, \quad (A.2.10)$$

$$\begin{aligned} f_{b15}^{(t\alpha R)} &= 4x_1x_3m_t(D_{13}^{(1)} - D_{23}^{(1)} + D_{25}^{(1)} + D_{26}^{(1)} - D_{39}^{(1)} + D_{310}^{(1)} \\ &\quad - 4x_1x_4m_{\tilde{g}}(D_0^{(1)} + D_{11}^{(1)} + D_{12}^{(1)} - D_{13}^{(1)} + D_{24}^{(1)} - D_{26}^{(1)}) \\ &\quad + 4x_2x_4m_t(D_{11}^{(1)} - D_{13}^{(1)} + D_{21}^{(1)} + D_{23}^{(1)} + D_{24}^{(1)} - 2D_{25}^{(1)} \\ &\quad - D_{26}^{(1)} + D_{34}^{(1)} + D_{39}^{(1)} - 2D_{310}^{(1)}), \end{aligned} \quad (A.2.11)$$

$$\begin{aligned} f_{b16}^{(t\alpha R)} &= 4x_1x_3m_t(-D_{25}^{(1)} + D_{26}^{(1)} - D_{35}^{(1)} + D_{37}^{(1)} - D_{39}^{(1)} + D_{310}^{(1)}) \\ &\quad + 4x_1x_4m_{\tilde{g}}(D_{11}^{(1)} - D_{12}^{(1)} + D_{21}^{(1)} - D_{24}^{(1)} - D_{25}^{(1)} + D_{26}^{(1)}) \\ &\quad - 4x_2x_4m_t(D_{21}^{(1)} - D_{24}^{(1)} - D_{25}^{(1)} + D_{26}^{(1)} + D_{31}^{(1)} \\ &\quad - D_{34}^{(1)} - 2D_{35}^{(1)} + D_{37}^{(1)} - D_{39}^{(1)} + 2D_{310}^{(1)}), \end{aligned} \quad (A.2.12)$$

$$\begin{aligned} f_{b17}^{(t\alpha R)} &= 4x_1x_3m_t(D_{37}^{(1)} - D_{39}^{(1)}) - 4x_1x_4m_{\tilde{g}}(D_{25}^{(1)} - D_{26}^{(1)}) \\ &\quad + 4x_2x_4m_t(D_{35}^{(1)} - D_{37}^{(1)} + D_{39}^{(1)} - D_{310}^{(1)}), \end{aligned} \quad (A.2.13)$$

$$\begin{aligned} f_{b18}^{(t\alpha R)} &= 4x_1x_3(-D_{22}^{(1)} + D_{24}^{(1)} - D_{25}^{(1)} + D_{26}^{(1)} + D_{34}^{(1)} \\ &\quad - D_{35}^{(1)} - D_{36}^{(1)} + D_{37}^{(1)} + D_{38}^{(1)} - D_{39}^{(1)}), \end{aligned} \quad (A.2.14)$$

$$f_{b19}^{(t\alpha R)} = 4x_1x_3(-D_{23}^{(1)} + D_{26}^{(1)} - D_{39}^{(1)} + D_{38}^{(1)}), \quad (A.2.15)$$

$$\begin{aligned} f_{b20}^{(t\alpha R)} = & 4x_1x_3m_t(-D_{23}^{(1)} - D_{39}^{(1)}) + 4x_1x_4m_{\tilde{g}}(D_{13}^{(1)} + D_{26}^{(1)}) \\ & + 4x_2x_4m_t(D_{23}^{(1)} - D_{25}^{(1)} + D_{39}^{(1)} - D_{310}^{(1)}), \end{aligned} \quad (A.2.16)$$

where we denote $D_i^{(1)}, D_{ij}^{(1)}, D_{ijk}^{(1)} = D_i, D_{ij}, D_{ijk}[-p_1, k_1, k_2, m_{\tilde{g}}, m_{\tilde{t}_1}, m_{\tilde{t}_1}, m_{\tilde{t}_1}]$.

The expressions of $f_{bk}^{t\beta R}$ are as follows:

$$f_{b1}^{(t\beta R)} = 2x_1x_3m_t(D_{27}^{(2)} + D_{313}^{(2)}) + 2x_1x_4m_{\tilde{g}}D_{27}^{(2)} - 2x_2x_4m_t(D_{27}^{(2)} + D_{311}^{(2)}), \quad (A.2.17)$$

$$f_{b2}^{(t\beta R)} = 2x_1x_3m_tD_{313}^{(2)} + 2x_1x_4m_{\tilde{g}}D_{27}^{(2)} - 2x_2x_4m_tD_{311}^{(2)}, \quad (A.2.18)$$

$$f_{b3}^{(t\beta R)} = 4x_1x_3(-D_{27}^{(2)} - D_{311}^{(2)} + D_{312}^{(2)}), \quad (A.2.19)$$

$$f_{b4}^{(t\beta R)} = 4x_1x_3(D_{312}^{(2)} - D_{313}^{(2)}), \quad (A.2.20)$$

$$\begin{aligned} f_{b5}^{(t\beta R)} = & 8x_1x_3(D_{27}^{(2)} + D_{311}^{(2)}) + 2x_1x_3m_{\tilde{g}}^2(D_0^{(2)} + D_{11}^{(2)}) \\ & + 2x_1x_3m_t^2(-D_{11}^{(2)} - D_{13}^{(2)} - 2D_{21}^{(2)} - D_{23}^{(2)} - D_{25}^{(2)} - D_{31}^{(2)} - D_{37}^{(2)}) \\ & + 2(x_2x_3 + x_1x_4)m_{\tilde{g}}m_t(D_0^{(2)} + D_{11}^{(2)}) - 2x_2x_4m_t^2(D_{11}^{(2)} - D_{13}^{(2)} + D_{21}^{(2)} - D_{25}^{(2)}) \\ & + 4x_1x_3k_1 \cdot p_1(D_{12}^{(2)} + 2D_{24}^{(2)} + D_{34}^{(2)}) \\ & + 4x_1x_3k_1 \cdot p_2(D_{13}^{(2)} + D_{25}^{(2)} + D_{26}^{(2)} + D_{310}^{(2)}) - 4x_1x_3p_1 \cdot p_2(D_{13}^{(2)} + 2D_{25}^{(2)} + D_{35}^{(2)}), \end{aligned} \quad (A.2.21)$$

$$\begin{aligned} f_{b6}^{(t\beta R)} = & 2x_1x_3m_{\tilde{g}}^2D_{13}^{(2)} \\ & - 2x_1x_3m_t^2(D_{23}^{(2)} + D_{25}^{(2)} + D_{33}^{(2)} + D_{35}^{(2)}) + 2(x_2x_3 + x_1x_4)m_{\tilde{g}}m_tD_{13}^{(2)} \\ & + 2x_2x_4m_t^2(D_{23}^{(2)} - D_{25}^{(2)}) + 4x_1x_3k_1 \cdot p_1(D_{26}^{(2)} + D_{310}^{(2)}) \\ & + 4x_1x_3k_1 \cdot p_2(D_{23}^{(2)} + D_{39}^{(2)}) - 4x_1x_3p_1 \cdot p_2(D_{23}^{(2)} + D_{37}^{(2)}) \\ & + 8x_1x_3D_{313}^{(2)}, \end{aligned} \quad (A.2.22)$$

$$f_{b7}^{(t\beta R)} = 2x_1x_3(D_{27}^{(2)} + D_{312}^{(2)}), \quad (A.2.23)$$

$$f_{b8}^{(t\beta R)} = 2x_1x_3D_{312}^{(2)}, \quad (A.2.24)$$

$$f_{b9}^{(t\beta R)} = 4x_1x_3(D_{12}^{(2)} - D_{13}^{(2)} + D_{22}^{(2)} + D_{24}^{(2)} - D_{25}^{(2)} - D_{26}^{(2)} + D_{36}^{(2)} - D_{310}^{(2)}), \quad (A.2.25)$$

$$f_{b10}^{(t\beta R)} = 4x_1x_3(D_{38}^{(2)} - D_{310}^{(2)}), \quad (A.2.26)$$

$$f_{b11}^{(t\beta R)} = f_{b12}^{(t\beta R)} = 0, \quad (A.2.27)$$

$$\begin{aligned} f_{b13}^{(t\beta R)} = & 2x_1x_3m_t(-D_{12}^{(2)} + D_{13}^{(2)} - D_{24}^{(2)} + D_{25}^{(2)}) + 2x_1x_4m_{\tilde{g}}(D_0^{(2)} + D_{11}^{(2)}) \\ & - 2x_2x_4m_t(D_{11}^{(2)} - D_{12}^{(2)} + D_{21}^{(2)} - D_{24}^{(2)}), \end{aligned} \quad (A.2.28)$$

$$f_{b14}^{(t\beta R)} = 2x_1x_3m_t(D_{23}^{(2)} - D_{26}^{(2)}) + 2x_1x_4m_{\tilde{g}}D_{13}^{(2)} - 2x_2x_4m_t(D_{25}^{(2)} - D_{26}^{(2)}), \quad (A.2.29)$$

$$\begin{aligned} f_{b15}^{(t\beta R)} = & 4x_1x_3m_t(D_{12}^{(2)} - D_{13}^{(2)} - D_{23}^{(2)} + D_{24}^{(2)} - D_{25}^{(2)} + D_{26}^{(2)} - D_{37}^{(2)} + D_{310}^{(2)}) \\ & + 4x_1x_4m_{\tilde{g}}(D_{12}^{(2)} - D_{13}^{(2)} + D_{24}^{(2)} - D_{25}^{(2)}) \\ & - 4x_2x_4m_t(D_{12}^{(2)} - D_{13}^{(2)} + 2D_{24}^{(2)} - 2D_{25}^{(2)} + D_{34}^{(2)} - D_{35}^{(2)}), \end{aligned} \quad (A.2.30)$$

$$\begin{aligned} f_{b16}^{(t\beta R)} = & 4x_1x_3m_t(D_{12}^{(2)} - D_{13}^{(2)} + D_{24}^{(2)} - 2D_{25}^{(2)} + D_{26}^{(2)} - D_{35}^{(2)} + D_{310}^{(2)}) \\ & + 4x_1x_4m_{\tilde{g}}(-D_0^{(2)} - 2D_{11}^{(2)} + D_{12}^{(2)} - D_{21}^{(2)} + D_{24}^{(2)}) \\ & + 4x_2x_4m_t(D_{11}^{(2)} - D_{12}^{(2)} + 2D_{21}^{(2)} - 2D_{24}^{(2)} + D_{31}^{(2)} - D_{34}^{(2)}), \end{aligned} \quad (A.2.31)$$

$$\begin{aligned} f_{b17}^{(t\beta R)} = & 4x_1x_3m_t(-D_{23}^{(2)} + D_{26}^{(2)} - D_{37}^{(2)} + D_{39}^{(2)}) + 4x_1x_4m_{\tilde{g}}(-D_{13}^{(2)} - D_{25}^{(2)} + D_{26}^{(2)}) \\ & + 4x_2x_4m_t(D_{25}^{(2)} - D_{26}^{(2)} + D_{35}^{(2)} - D_{310}^{(2)}), \end{aligned} \quad (A.2.32)$$

$$f_{b18}^{(t\beta R)} = 4x_1x_3(D_{22}^{(2)} - D_{24}^{(2)} - D_{34}^{(2)} + D_{36}^{(2)}), \quad (A.2.33)$$

$$f_{b19}^{(t\beta R)} = 4x_1x_3(-D_{23}^{(2)} + D_{26}^{(2)} + D_{38}^{(2)} - D_{39}^{(2)}), \quad (A.2.34)$$

$$\begin{aligned} f_{b20}^{(t\beta R)} = & 4x_1x_3m_t(-D_{23}^{(2)} + D_{26}^{(2)} - D_{33}^{(2)} + D_{39}^{(2)}) + 4x_1x_4m_{\tilde{g}}(-D_{23}^{(2)} + D_{26}^{(2)}) \\ & + 4x_2x_4m_t(D_{23}^{(2)} - D_{26}^{(2)} + D_{37}^{(2)} - D_{310}^{(2)}), \end{aligned} \quad (A.2.35)$$

where $D_i^{(2)}, D_{ij}^{(2)}, D_{ijk}^{(2)} = D_i, D_{ij}, D_{ijk}[-p_1, k_1, -p_2, m_{\tilde{g}}, m_{\tilde{t}_1}, m_{\tilde{t}_1}, m_{\tilde{g}}]$.

We express $f_{bk}^{t\gamma R}$ as:

$$\begin{aligned}
f_{b1}^{(t\gamma R)} = & 2x_1x_3m_t(D_{27}^{(3)} + 2D_{313}^{(3)}) + x_1x_3m_t m_{\tilde{g}}^2(D_0^{(3)} + D_{13}^{(3)}) \\
& -x_1x_3m_t^3(D_0^{(3)} + 2D_{11}^{(3)} - D_{13}^{(3)} + D_{21}^{(3)} + 2D_{33}^{(3)} + 2D_{35}^{(3)} - 2D_{37}^{(3)}) \\
& +2x_1x_4m_{\tilde{g}}D_{27}^{(3)} + x_1x_4m_{\tilde{g}}^3D_0^{(3)} \\
& -x_1x_4m_t^2m_{\tilde{g}}(D_0^{(3)} + 2D_{11}^{(3)} - 2D_{13}^{(3)} + D_{21}^{(3)} + 2D_{23}^{(3)} - 2D_{25}^{(3)}) \\
& +2x_2x_4m_t(D_{27}^{(3)} + 2D_{311}^{(3)} - 2D_{313}^{(3)}) + x_2x_4m_t m_{\tilde{g}}^2(D_{11}^{(3)} - D_{13}^{(3)}) \\
& -x_2x_4m_t^3(D_{11}^{(3)} - D_{13}^{(3)} + 2D_{21}^{(3)} + 2D_{23}^{(3)} - 4D_{25}^{(3)} + D_{31}^{(3)} - 2D_{33}^{(3)} - 3D_{35}^{(3)} + 4D_{37}^{(3)}) \\
& +2x_1x_3m_t k_1 \cdot p_1(D_{12}^{(3)} - D_{13}^{(3)} - D_{23}^{(3)} + D_{24}^{(3)} + D_{33}^{(3)} - D_{37}^{(3)} - D_{39}^{(3)} + D_{310}^{(3)}) \\
& +2x_1x_4m_{\tilde{g}}k_1 \cdot p_1(D_{11}^{(3)} + D_{12}^{(3)} - 2D_{13}^{(3)} + D_{23}^{(3)} + D_{24}^{(3)} - D_{25}^{(3)} - D_{26}^{(3)}) \\
& +2x_2x_4m_t k_1 \cdot p_1(D_{11}^{(3)} - D_{13}^{(3)} + D_{21}^{(3)} + 2D_{23}^{(3)}) \\
& +D_{24}^{(3)} - 3D_{25}^{(3)} - D_{26}^{(3)} - D_{33}^{(3)} + D_{34}^{(3)} - D_{35}^{(3)} + 2D_{37}^{(3)} + D_{39}^{(3)} - 2D_{310}^{(3)}) \\
& +2x_1x_3m_t k_1 \cdot p_2(-D_{13}^{(3)} - D_{26}^{(3)} + D_{33}^{(3)} - D_{39}^{(3)}) \\
& +2x_1x_4m_{\tilde{g}}k_1 \cdot p_2(-D_{13}^{(3)} + D_{23}^{(3)} - D_{26}^{(3)}) \\
& +2x_2x_4m_t k_1 \cdot p_2(D_{23}^{(3)} - D_{25}^{(3)} - D_{33}^{(3)} + D_{37}^{(3)} + D_{39}^{(3)} - D_{310}^{(3)}) \\
& +2x_1x_3m_t p_1 \cdot p_2(D_{13}^{(3)} + D_{25}^{(3)} - D_{33}^{(3)} + D_{37}^{(3)}) \\
& +2x_1x_4m_{\tilde{g}}p_1 \cdot p_2(D_{13}^{(3)} - D_{23}^{(3)} + D_{25}^{(3)}) \\
& +2x_2x_4m_t p_1 \cdot p_2(-D_{23}^{(3)} + D_{25}^{(3)} + D_{33}^{(3)} + D_{35}^{(3)} - D_{37}^{(3)}), \tag{A.2.36}
\end{aligned}$$

$$f_{b2}^{(t\gamma R)} = -2x_1x_4m_{\tilde{g}}D_{27}^{(3)} - 2x_1x_3m_tD_{313}^{(3)} - 2x_2x_4m_t(D_{27}^{(3)} + D_{311}^{(3)} - D_{313}^{(3)}), \tag{A.2.37}$$

$$\begin{aligned}
f_{b3}^{(t\gamma R)} = & 4x_1x_3(D_{27}^{(3)} + 2D_{311}^{(3)} + D_{312}^{(3)} - 3D_{313}^{(3)}) + 2x_1x_3m_{\tilde{g}}^2(-D_0^{(3)} + D_{11}^{(3)} - D_{13}^{(3)}) \\
& +2x_1x_3m_t^2(D_{13}^{(3)} - D_{21}^{(3)} + 2D_{25}^{(3)} - D_{31}^{(3)} + 2D_{33}^{(3)} + 3D_{35}^{(3)} - 4D_{37}^{(3)}) \\
& -2x_2x_3m_t m_{\tilde{g}}D_0^{(3)} - 2x_1x_4m_t m_{\tilde{g}}D_0^{(3)} - 2x_2x_4m_t^2(D_0^{(3)} + D_{11}^{(3)}) \\
& +4x_1x_3k_1 \cdot p_1(D_{23}^{(3)} + D_{24}^{(3)} - D_{25}^{(3)} - D_{26}^{(3)}) \\
& -D_{33}^{(3)} + D_{34}^{(3)} - D_{35}^{(3)} + 2D_{37}^{(3)} + D_{39}^{(3)} - 2D_{310}^{(3)}) \\
& +4x_1x_3k_1 \cdot p_2(-D_{25}^{(3)} + D_{26}^{(3)} - D_{33}^{(3)} + D_{37}^{(3)} + D_{39}^{(3)} - D_{310}^{(3)}) \\
& +4x_1x_3p_1 \cdot p_2(D_{33}^{(3)} + D_{35}^{(3)} - 2D_{37}^{(3)}), \tag{A.2.38}
\end{aligned}$$

$$\begin{aligned}
f_{b4}^{(t\gamma R)} = & 4x_1x_3D_{312}^{(3)} - 2x_1x_3m_{\tilde{g}}^2D_0^{(3)} \\
& +2x_1x_3m_t^2(D_{11}^{(3)} + D_{21}^{(3)} + 2D_{23}^{(3)} - 2D_{25}^{(3)}) \\
& -2x_2x_3m_t m_{\tilde{g}}D_0^{(3)} - 2x_1x_4m_t m_{\tilde{g}}D_0^{(3)} \\
& -2x_2x_4m_t^2(D_0^{(3)} + D_{11}^{(3)}) + 4x_1x_3k_1 \cdot p_1(-D_{23}^{(3)} + D_{25}^{(3)}) \\
& +4x_1x_3k_1 \cdot p_2(-D_{23}^{(3)} + D_{26}^{(3)}) + 4x_1x_3p_1 \cdot p_2(D_{23}^{(3)} - D_{25}^{(3)}), \tag{A.2.39}
\end{aligned}$$

$$\begin{aligned}
f_{b5}^{(t\gamma R)} = & 4x_1x_3(-D_{311}^{(3)} + D_{313}^{(3)}) + 2x_1x_3m_{\tilde{g}}^2D_0^{(3)} \\
& -2x_1x_3m_t^2(D_{13}^{(3)} + D_{25}^{(3)}) + 2x_2x_3m_tm_{\tilde{g}}(D_0^{(3)} + D_{11}^{(3)} - D_{13}^{(3)}) \\
& +2x_1x_4m_tm_{\tilde{g}}(D_0^{(3)} + D_{11}^{(3)} - D_{13}^{(3)}) \\
& +2x_2x_4m_t^2(D_0^{(3)} + 2D_{11}^{(3)} - D_{13}^{(3)} + D_{21}^{(3)} - D_{25}^{(3)}) \\
& +4x_1x_3k_1 \cdot p_2(D_{25}^{(3)} - D_{26}^{(3)}), \tag{A.2.40}
\end{aligned}$$

$$\begin{aligned}
f_{b6}^{(t\gamma R)} = & -8x_1x_3D_{313}^{(3)} - 2x_1x_3m_{\tilde{g}}^2D_{13}^{(3)} \\
& +2x_1x_3m_t^2(D_{25}^{(3)} + 2D_{33}^{(3)} + D_{35}^{(3)} - 2D_{37}^{(3)}) - 2x_2x_3m_tm_{\tilde{g}}D_{13}^{(3)} \\
& -2x_1x_4m_tm_{\tilde{g}}D_{13}^{(3)} - 2x_2x_4m_t^2(D_{13}^{(3)} + D_{25}^{(3)}) \\
& +4x_1x_3k_1 \cdot p_1(D_{23}^{(3)} - D_{25}^{(3)} - D_{33}^{(3)} + D_{37}^{(3)} + D_{39}^{(3)} - D_{310}^{(3)}) \\
& +4x_1x_3k_1 \cdot p_2(-D_{33}^{(3)} + D_{39}^{(3)}) + 4x_1x_3p_1 \cdot p_2(D_{33}^{(3)} - D_{37}^{(3)}), \tag{A.2.41}
\end{aligned}$$

$$\begin{aligned}
f_{b7}^{(t\gamma R)} = & -4x_1x_3(D_{312}^{(3)} - D_{313}^{(3)}) + x_1x_3m_{\tilde{g}}^2(D_0^{(3)} - D_{12}^{(3)} + D_{13}^{(3)}) \\
& +x_1x_3m_t^2(-D_{11}^{(3)} + D_{12}^{(3)} - D_{13}^{(3)} - D_{21}^{(3)}) \\
& +2D_{24}^{(3)} - 2D_{26}^{(3)} - 2D_{33}^{(3)} + D_{34}^{(3)} - D_{35}^{(3)} + 2D_{37}^{(3)} + 2D_{39}^{(3)} - 2D_{310}^{(3)} \\
& +(x_2x_3 + x_1x_4)m_tm_{\tilde{g}}D_0^{(3)} + x_2x_4m_t^2(D_0^{(3)} + D_{11}^{(3)}) \\
& +2x_1x_3k_1 \cdot p_1(-D_{22}^{(3)} - D_{23}^{(3)} + 2D_{26}^{(3)} + D_{33}^{(3)} - D_{36}^{(3)} - D_{37}^{(3)} + D_{38}^{(3)} - 2D_{39}^{(3)} + 2D_{310}^{(3)}) \\
& +2x_1x_3k_1 \cdot p_2(D_{33}^{(3)} + D_{38}^{(3)} - 2D_{39}^{(3)}) \\
& +2x_1x_3p_1 \cdot p_2(D_{25}^{(3)} - D_{26}^{(3)} - D_{33}^{(3)} + D_{37}^{(3)} + D_{39}^{(3)} - D_{310}^{(3)}), \tag{A.2.42}
\end{aligned}$$

$$f_{b8}^{(t\gamma R)} = 2x_1x_3(D_{27}^{(3)} + D_{312}^{(3)} - D_{313}^{(3)}), \tag{A.2.43}$$

$$f_{b9}^{(t\gamma R)} = 4x_1x_3(D_{22}^{(3)} + D_{23}^{(3)} - D_{25}^{(3)} - D_{26}^{(3)} + D_{36}^{(3)} - D_{38}^{(3)} + D_{39}^{(3)} - D_{310}^{(3)}), \tag{A.2.44}$$

$$f_{b10}^{(t\gamma R)} = 4x_1x_3(D_{25}^{(3)} - D_{26}^{(3)} - D_{37}^{(3)} - D_{38}^{(3)} + D_{39}^{(3)} + D_{310}^{(3)}), \tag{A.2.45}$$

$$\begin{aligned}
f_{b11}^{(t\gamma R)} = & 2x_1x_3m_t(-D_{25}^{(3)} + D_{26}^{(3)}) + 2x_1x_4m_{\tilde{g}}(-D_{11}^{(3)} + D_{12}^{(3)}) \\
& +2x_2x_4m_t(-D_{11}^{(3)} + D_{12}^{(3)} - D_{21}^{(3)} + D_{24}^{(3)} + D_{25}^{(3)} - D_{26}^{(3)}), \tag{A.2.46}
\end{aligned}$$

$$\begin{aligned}
f_{b12}^{(t\gamma R)} = & 2x_1x_3m_t(D_{13}^{(3)} + D_{26}^{(3)}) + 2x_1x_4m_{\tilde{g}}D_{12}^{(3)} \\
& +2x_2x_4m_t(D_{12}^{(3)} - D_{13}^{(3)} + D_{24}^{(3)} - D_{26}^{(3)}), \tag{A.2.47}
\end{aligned}$$

$$\begin{aligned}
f_{b13}^{(t\gamma R)} = & 2x_1x_3m_t(D_{12}^{(3)} - D_{13}^{(3)} + D_{24}^{(3)} - D_{26}^{(3)}) + 2x_1x_4m_{\tilde{g}}(D_{11}^{(3)} - D_{13}^{(3)}) \\
& +2x_2x_4m_t(D_{11}^{(3)} - D_{12}^{(3)} + D_{21}^{(3)} - D_{24}^{(3)} - D_{25}^{(3)} + D_{26}^{(3)}), \tag{A.2.48}
\end{aligned}$$

$$\begin{aligned}
f_{b14}^{(t\gamma R)} = & -2x_1x_3m_t(D_{13}^{(3)} + D_{26}^{(3)}) - 2x_1x_4m_{\tilde{g}}D_{13}^{(3)} \\
& +2x_2x_4m_t(-D_{25}^{(3)} + D_{26}^{(3)}), \tag{A.2.49}
\end{aligned}$$

$$\begin{aligned}
f_{b15}^{(t\gamma R)} = & -4x_1x_3m_t(D_{12}^{(3)} - D_{23}^{(3)} + D_{24}^{(3)} + D_{25}^{(3)} - D_{39}^{(3)} + D_{310}^{(3)}) \\
& + 4x_1x_4m_{\tilde{g}}(-D_{11}^{(3)} - D_{12}^{(3)} + D_{13}^{(3)} - D_{24}^{(3)} + D_{26}^{(3)}) \\
& + 4x_2x_4m_t(-D_{11}^{(3)} + D_{13}^{(3)} - D_{21}^{(3)} - D_{23}^{(3)} \\
& - D_{24}^{(3)} + 2D_{25}^{(3)} + D_{26}^{(3)} - D_{34}^{(3)} - D_{39}^{(3)} + 2D_{310}^{(3)}),
\end{aligned} \tag{A.2.50}$$

$$\begin{aligned}
f_{b16}^{(t\gamma R)} = & -4x_1x_3m_t(D_{12}^{(3)} - D_{13}^{(3)} + D_{24}^{(3)} - D_{25}^{(3)} - D_{35}^{(3)} + D_{37}^{(3)} - D_{39}^{(3)} + D_{310}^{(3)}) \\
& + 4x_1x_4m_{\tilde{g}}(-D_{12}^{(3)} + D_{13}^{(3)} + D_{21}^{(3)} - D_{24}^{(3)} - D_{25}^{(3)} + D_{26}^{(3)}) \\
& + 4x_2x_4m_t(D_{21}^{(3)} - D_{24}^{(3)} - D_{25}^{(3)} + D_{26}^{(3)} \\
& + D_{31}^{(3)} - D_{34}^{(3)} - 2D_{35}^{(3)} + D_{37}^{(3)} - D_{39}^{(3)} + 2D_{310}^{(3)}),
\end{aligned} \tag{A.2.51}$$

$$\begin{aligned}
f_{b17}^{(t\gamma R)} = & 4x_1x_3m_t(D_{13}^{(3)} + D_{26}^{(3)} - D_{37}^{(3)} + D_{39}^{(3)}) \\
& + 4x_1x_4m_{\tilde{g}}(D_{13}^{(3)} - D_{25}^{(3)} + D_{26}^{(3)}) + 4x_2x_4m_t(-D_{35}^{(3)} + D_{37}^{(3)} - D_{39}^{(3)} + D_{310}^{(3)}),
\end{aligned} \tag{A.2.52}$$

$$\begin{aligned}
f_{b18}^{(t\gamma R)} = & 4x_1x_3(D_{22}^{(3)} - D_{24}^{(3)} + D_{25}^{(3)} - D_{26}^{(3)} - D_{34}^{(3)} + D_{35}^{(3)} + D_{36}^{(3)} \\
& - D_{37}^{(3)} - D_{38}^{(3)} + D_{39}^{(3)}),
\end{aligned} \tag{A.2.53}$$

$$f_{b19}^{(t\gamma R)} = 4x_1x_3(D_{23}^{(3)} - D_{26}^{(3)} - D_{38}^{(3)} + D_{39}^{(3)}), \tag{A.2.54}$$

$$\begin{aligned}
f_{b20}^{(t\gamma R)} = & 4x_1x_3m_t(D_{13}^{(3)} + D_{23}^{(3)} + D_{26}^{(3)} + D_{39}^{(3)}) \\
& + 4x_1x_4m_{\tilde{g}}(D_{13}^{(3)} + D_{26}^{(3)}) + 4x_2x_4m_t(-D_{23}^{(3)} + D_{25}^{(3)} - D_{39}^{(3)} + D_{310}^{(3)}),
\end{aligned} \tag{A.2.55}$$

where $D_i^{(3)}, D_{ij}^{(3)}, D_{ijk}^{(3)} = D_i, D_{ij}, D_{ijk}[-p_1, k_1, k_2, m_{\tilde{t}_1}, m_{\tilde{g}}, m_{\tilde{g}}, m_{\tilde{g}}]$

The $f_{bk}^{t\delta R}$ are written explicitly as:

$$\begin{aligned}
f_{b1}^{(t\delta R)} = & f_{b2}^{(t\delta R)} \\
& + \frac{1}{2}((x_1x_3m_t(C_{11} - C_{12}) \\
& + x_2x_4m_tC_{12} - x_2x_3m_{\tilde{g}}C_0)[-p_1, p_1 + p_2, m_{\tilde{g}}, m_{\tilde{t}_1}, m_{\tilde{t}_1}])
\end{aligned} \tag{A.2.56}$$

$$f_{bi}^{(t\delta R)} = 0, (i = 3, 4, \dots, 20). \tag{A.2.57}$$

All the definitions of loop integral functions B, C and D used in our paper can be found in Ref.[10]. The numerical calculation of the vector and tensor loop integral functions can be traced back to four scalar loop integrals A_0, B_0, C_0, D_0 in Ref. [11].

References

- [1] H.E. Haber and G.L. Kane, Phys. Rep. **117**, 75(1985); J.F. Gunion and H.E. Haber, Nucl. Phys. **B272**, 1(1986).
- [2] P.C. Bhat, for the D0 collaboration, talk presented at the Wine and Cheese Seminar at Fermilab, February 1997
- [3] M. Glück, J.F. Owens and E. Reya, Phys. Rev. D17,2324(1978); B.L. Combridge, Nucl.Phys.**B151**,429(1979); H. Georgi, *et al.*, Ann. Phys.(N.Y.)114,273(1978).
- [4] P. Nason, S. Dawson and R.K. Ellis, Nucl.Phys.B303,607(1988); G. Altarelli, M. Diemoz, G. Martinelli and P.Nason, Nucl.Phys. **B308**,724(1988); W. Beenakker, H. Kujif, W.L. van Neerven and J. Smith, Phys. Rev. **D40**,54(1989).
- [5] C. Li, B. Hu, J. Yang and C. Hu, Phys. Rev. **D52**,5014(1995); Z. Sullivan, Reprint: hep-ph/9611302.
- [6] H.Y. Zhou, C.S. Li, Phys. Rev. **D55**,4421(1997);
- [7] A. Bartl, E Christova and W. Majerotto, Nucl. Phys. **B460** (1996)235.
- [8] T. Gehrmann and W.J. Stirling,Z. Phys. C65(1995)461; S.J. Brodsky, M. Burkardt and I. Schmidt, Nucl. Phys. **B441**(1995)197 and the references therein.
- [9] W.Beenaker,R.Höpker,T.Plehn and P.M.Zerwas, DESY.96-178, October 1996
- [10] Bernd A. Kniehl, Phys. Rep. 240(1994)211.

[11] G. Passarino and M. Veltman, Nucl. Phys. **B160**, 151(1979).

Figure Captions

Fig.1 Feynman diagrams at the tree-level and one-loop level in Supersymmetric QCD for the $gg \rightarrow t\bar{t}$ process. Fig.1 (a): tree level diagrams. Fig.1 (b.1): self-energy diagrams (top-quark and gluon). Fig.1 (b.2): vertex diagrams (tri-gluon and gluon-top-top). Fig.1 (b.3): box diagrams(only t-channel). dashed lines represent \tilde{t}_1, \tilde{t}_2 for Fig.1 (b).

Fig.2 $m_{\tilde{g}} = 200 \text{ GeV}$, $m_{\tilde{t}_1} = 250 \text{ GeV}$, $m_{\tilde{t}_2} = 450 \text{ GeV}$ and $\theta = \phi = 45^\circ$. (a) relative corrections to polarized and unpolarized cross section of the $t\bar{t}$ production process in pp colliders as a function of \sqrt{s} , solid line for the MSSM QCD correction with unpolarized protons, dashed line for the MSSM QCD correction with *proton(+)proton(+)polarization*, dot line for the MSSM QCD correction with *proton(−)proton(−)polarization* and dot-dashed line for the MSSM QCD correction with *proton(+)proton(−)polarization*; (b) the CP-violating parameter ξ_{CP} as a function of \sqrt{s} .

Fig.3 $m_{\tilde{g}} = 200 \text{ GeV}$, $m_{\tilde{t}_1} = 250 \text{ GeV}$, $m_{\tilde{t}_2} = 450 \text{ GeV}$ and $\theta = \phi = 45^\circ$. (a) relative corrections to cross section of the $t\bar{t}$ production subprocess $\delta\hat{\sigma}_{\pm\pm}$ as a function of $\sqrt{\hat{s}}$, solid line for the MSSM QCD correction with *gluon(+)gluon(+)polarization* and dashed line for the MSSM QCD correction with *gluon(−)gluon(−)polarization*. (b) the CP-violating parameter ξ_{CP} of the subprocess as a function of $\sqrt{\hat{s}}$. (c) relative corrections to cross section of the subprocess $\delta\hat{\sigma}_{+-}$ as a function of $\sqrt{\hat{s}}$,

Fig.4 $m_{\tilde{t}_1} = 100 \text{ GeV}$, $m_{\tilde{t}_2} = 450 \text{ GeV}$, $\sqrt{\hat{s}} = 500 \text{ GeV}$ and $\theta = \phi = 45^\circ$. (a) cross section of the $t\bar{t}$ production subprocess via gg fusion $\hat{\sigma}_{\pm\pm}$ as a function of $m_{\tilde{g}}$, solid line for the MSSM QCD correction with *gluon(+)gluon(+)polarization* and dashed line for

the MSSM QCD correction with $gluon(-)gluon(-)$ polarization. (b) the CP-violating parameter ξ_{CP} of the subprocess as a function of $m_{\tilde{g}}$.

Fig.5 $m_{\tilde{g}} = 200 \text{ GeV}$, $m_{\tilde{t}_2} = 450 \text{ GeV}$, $\sqrt{\hat{s}} = 500 \text{ GeV}$ and $\theta = \phi = 45^\circ$. (a) relative corrections to cross section of the $t\bar{t}$ production subprocess via gg fusion $\delta\hat{\sigma}_{\pm\pm}$ as a function of $m_{\tilde{t}_1}$, solid line for the MSSM QCD correction with $gluon(+)+gluon(+)$ polarization and dashed line for the MSSM QCD correction with $gluon(-)+gluon(-)$ polarization. (b) the CP-violating parameter ξ_{CP} of the subprocess as a function of $m_{\tilde{t}_1}$.

Fig.6 $m_{\tilde{g}} = 200 \text{ GeV}$, $m_{\tilde{t}_1} = 100 \text{ GeV}$ and $\sqrt{\hat{s}} = 500 \text{ GeV}$ and $\theta = \phi = 45^\circ$. (a) relative corrections to cross section of the $t\bar{t}$ production subprocess via gg fusion $\delta\hat{\sigma}_{\pm\pm}$ as a function of $m_{\tilde{t}_2}$, solid line for the MSSM QCD correction with $gluon(+)+gluon(+)$ polarization and dashed line for the MSSM QCD correction with $gluon(-)+gluon(-)$ polarization. (b) the CP-violating parameter ξ_{CP} of the subprocess as a function of $m_{\tilde{t}_2}$.

Fig.7 $m_{\tilde{g}} = 200 \text{ GeV}$, $m_{\tilde{t}_1} = 150 \text{ GeV}$, $m_{\tilde{t}_2} = 450 \text{ GeV}$, $\sqrt{\hat{s}} = 500 \text{ GeV}$ and $\theta = 45^\circ$. (a) relative corrections to cross section of the $t\bar{t}$ production subprocess via gg fusion $\delta\hat{\sigma}_{\pm\pm}$ as a function of ϕ , solid line for the MSSM QCD correction with $gluon(+)+gluon(+)$ polarization and dashed line for the MSSM QCD correction with $gluon(-)+gluon(-)$ polarization. (b) the CP-violating parameter ξ_{CP} of the subprocess as a function of ϕ .

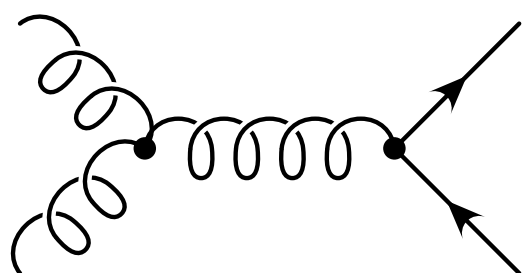
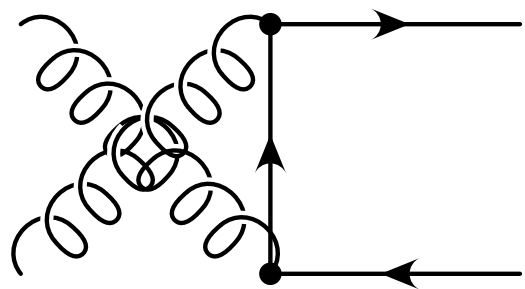
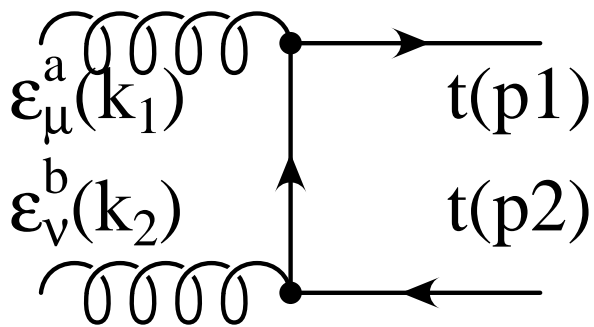


Fig.1 (a)

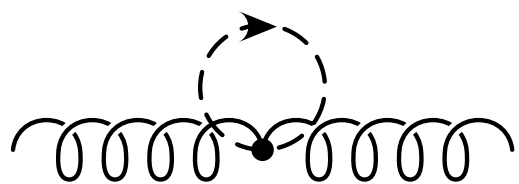
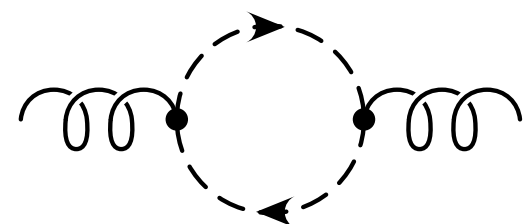
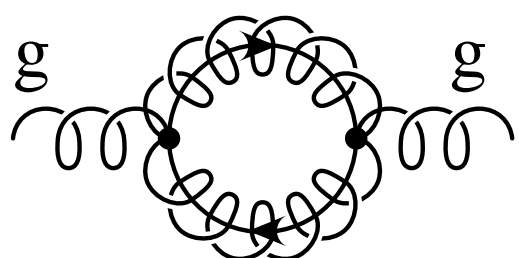
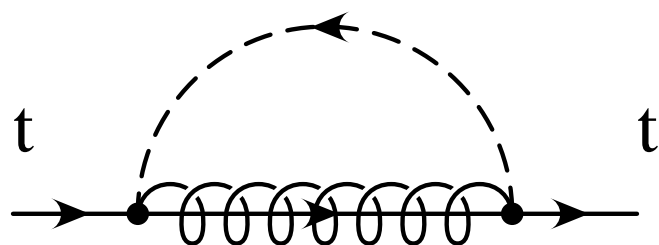


Fig.1 (b-1)

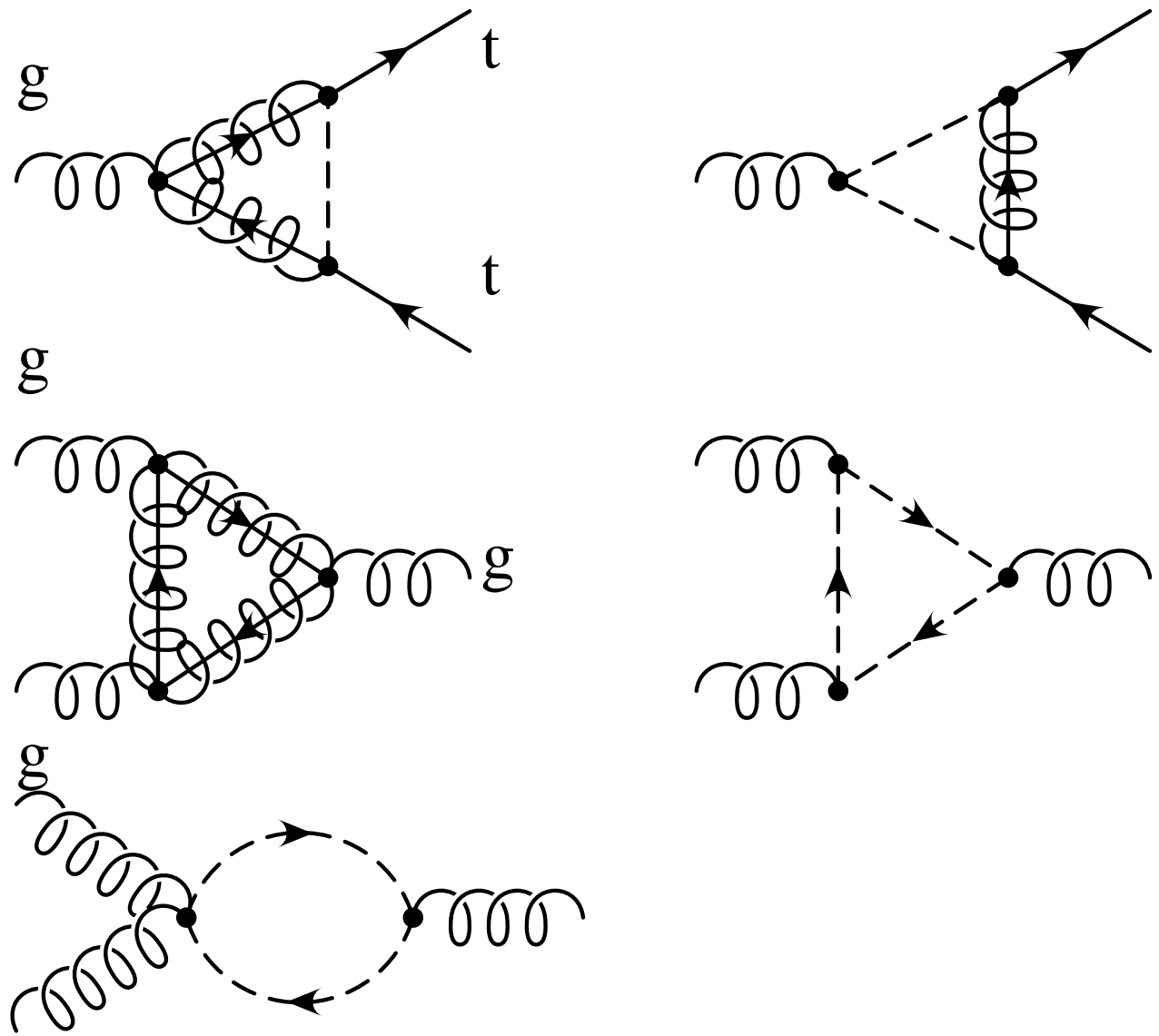


Fig.1 (b-2)

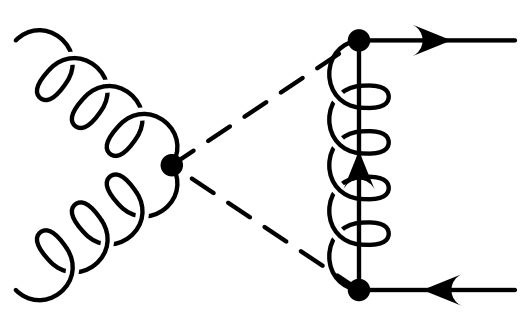
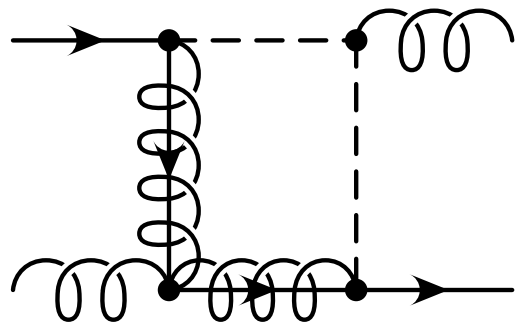
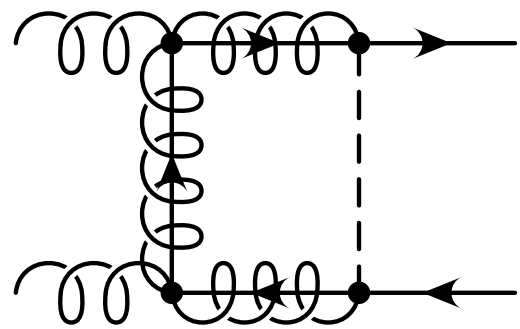
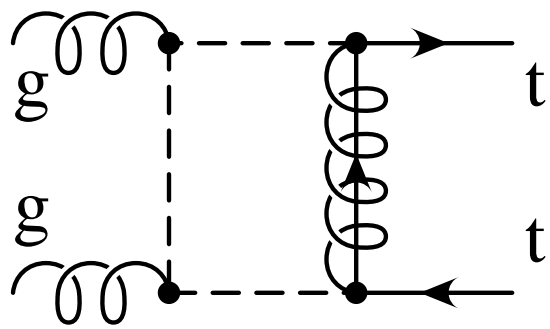


Fig.1 (b-3)

Fig.2 (a)

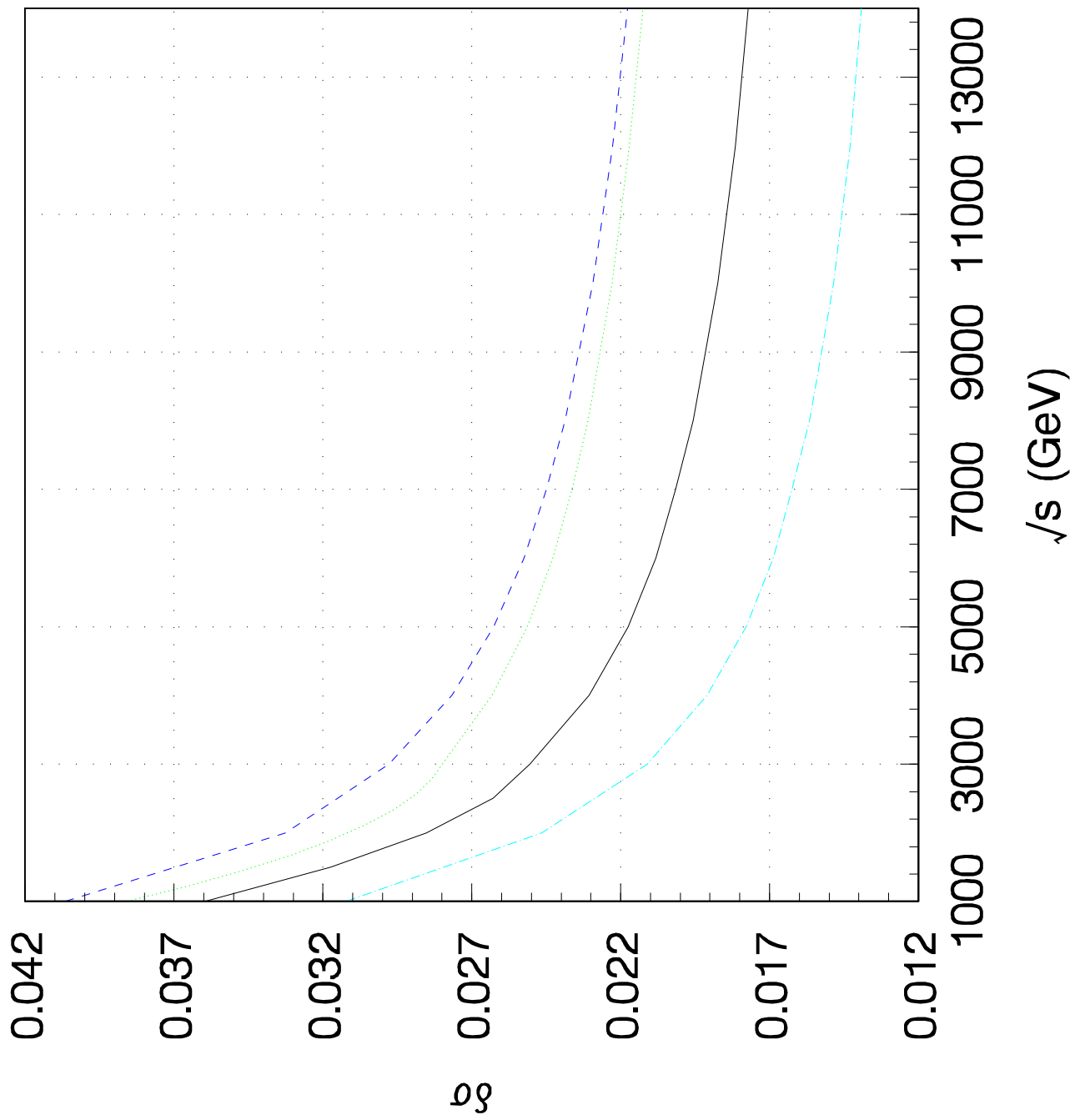


Fig.2 (b)

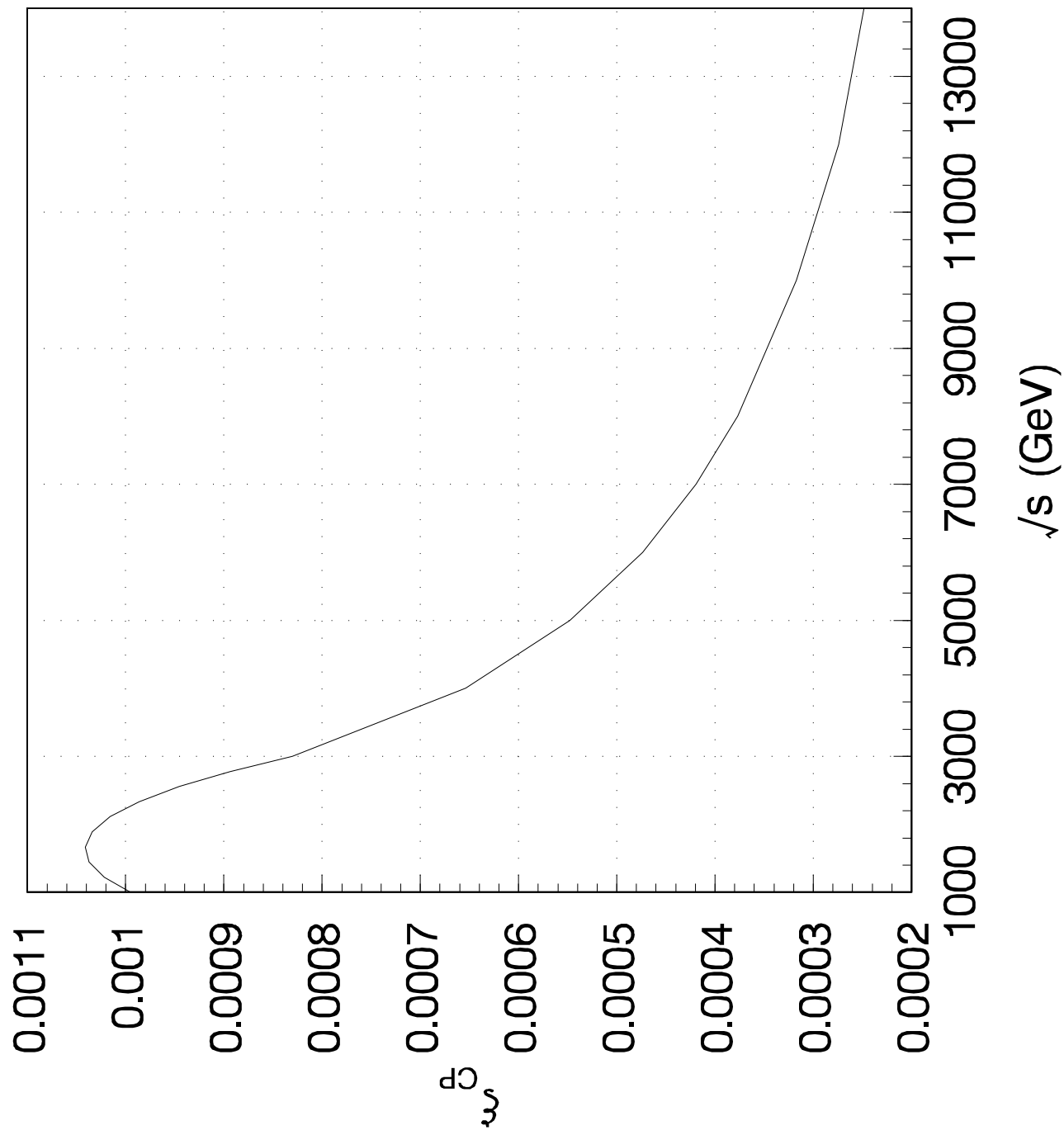


Fig. 3 (a)

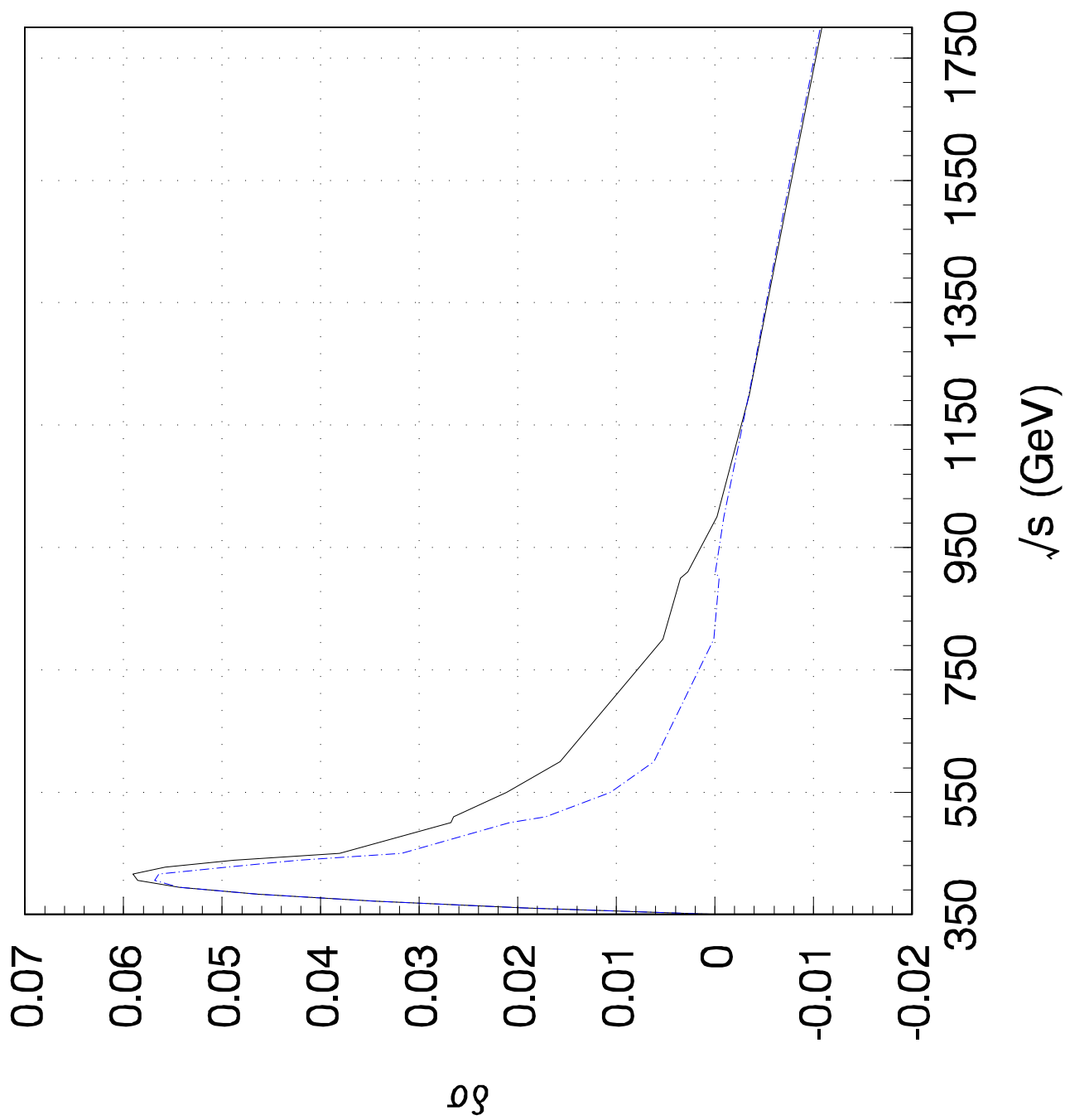


Fig.3 (b)

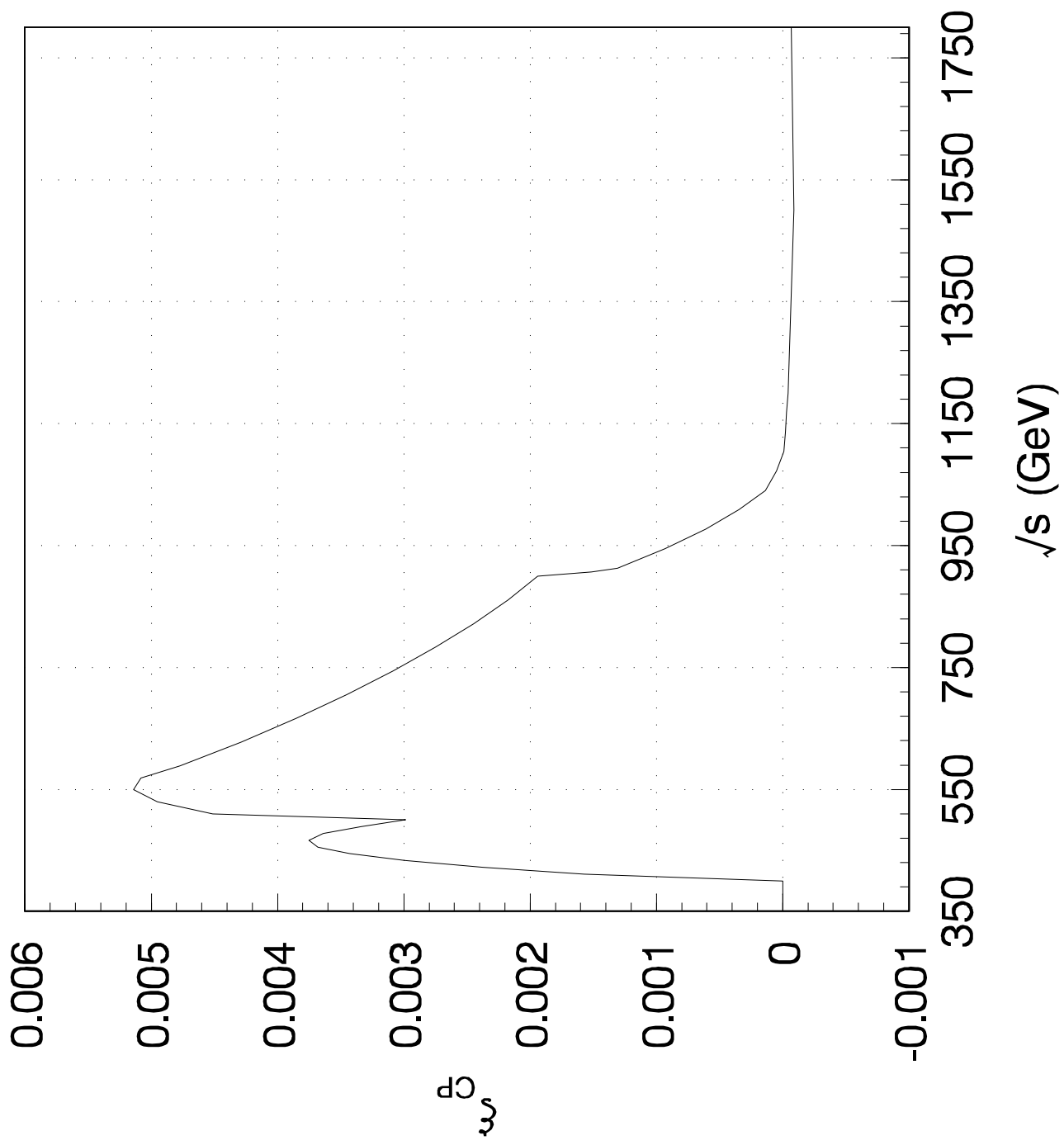


Fig. 3 (c)

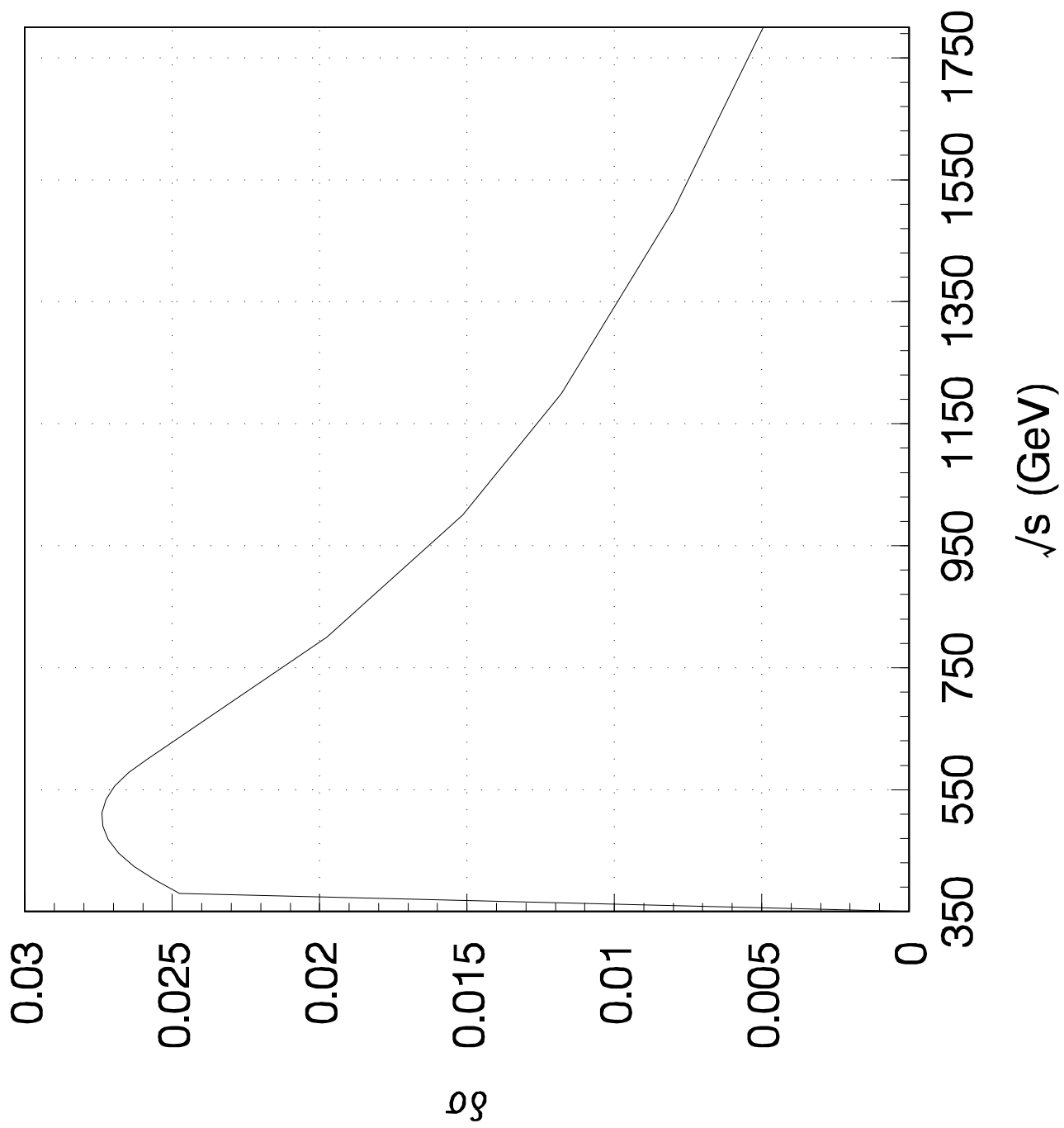


Fig.4 (a)

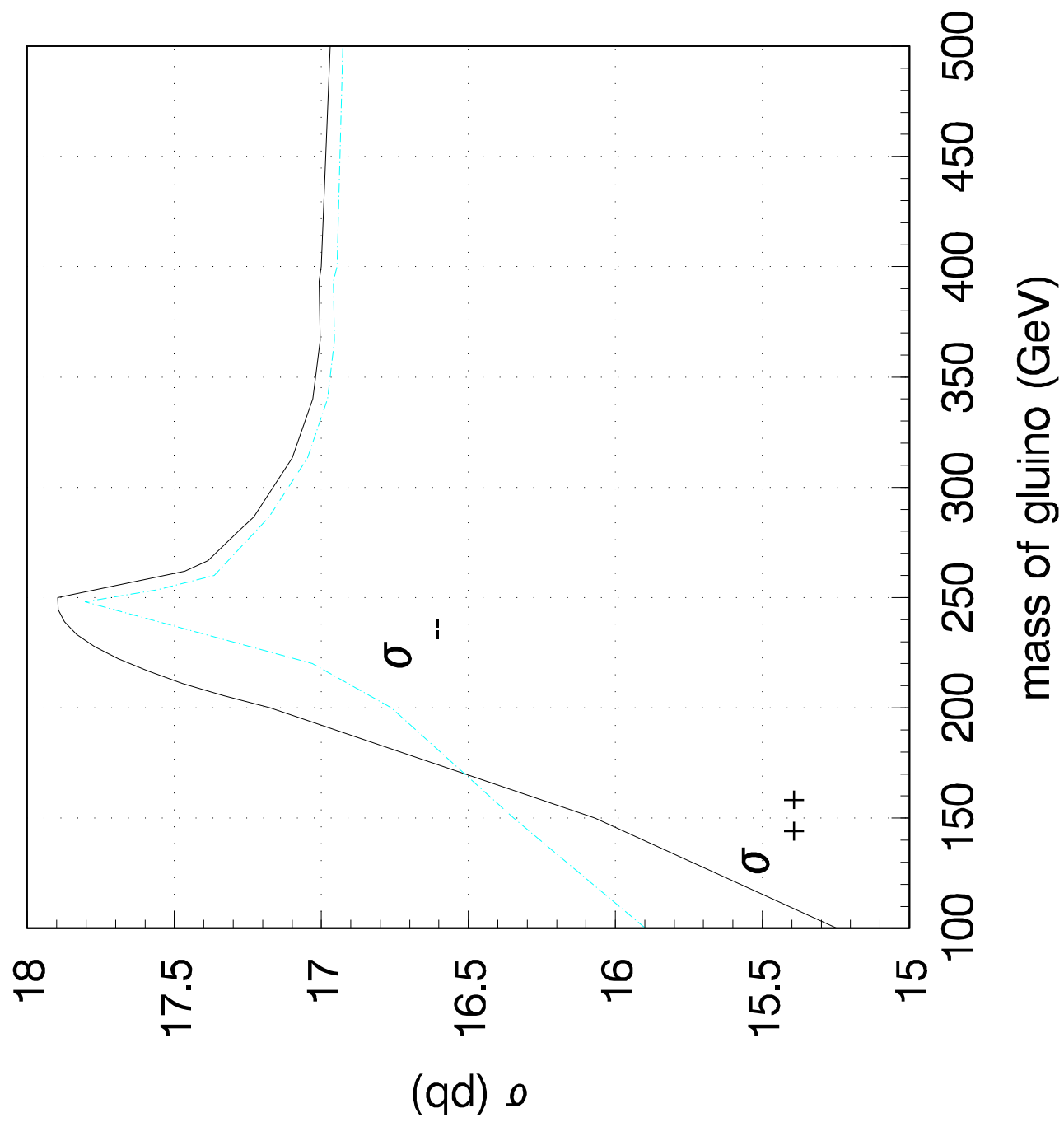


Fig. 4 (b)

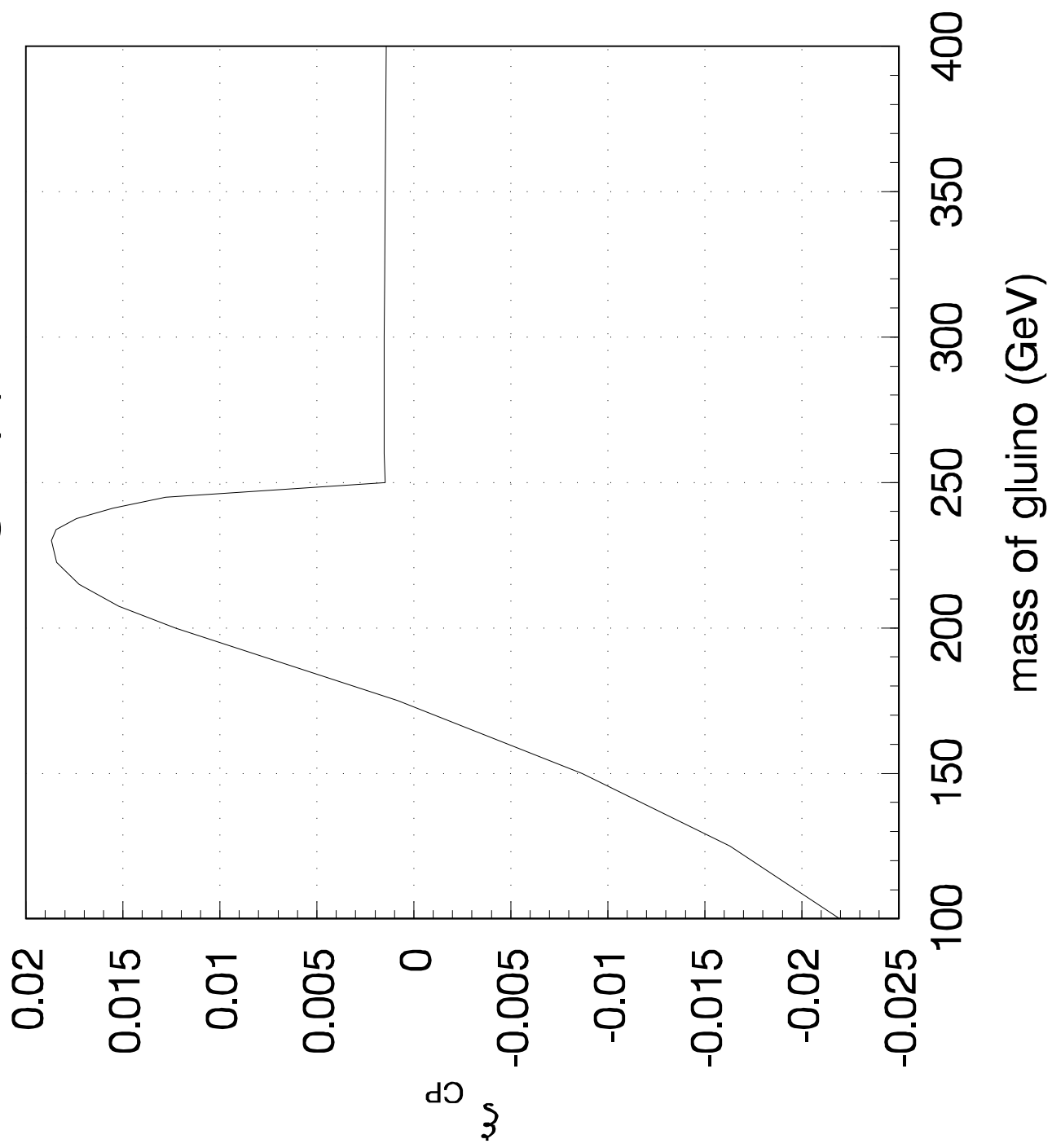


Fig.5 (a)

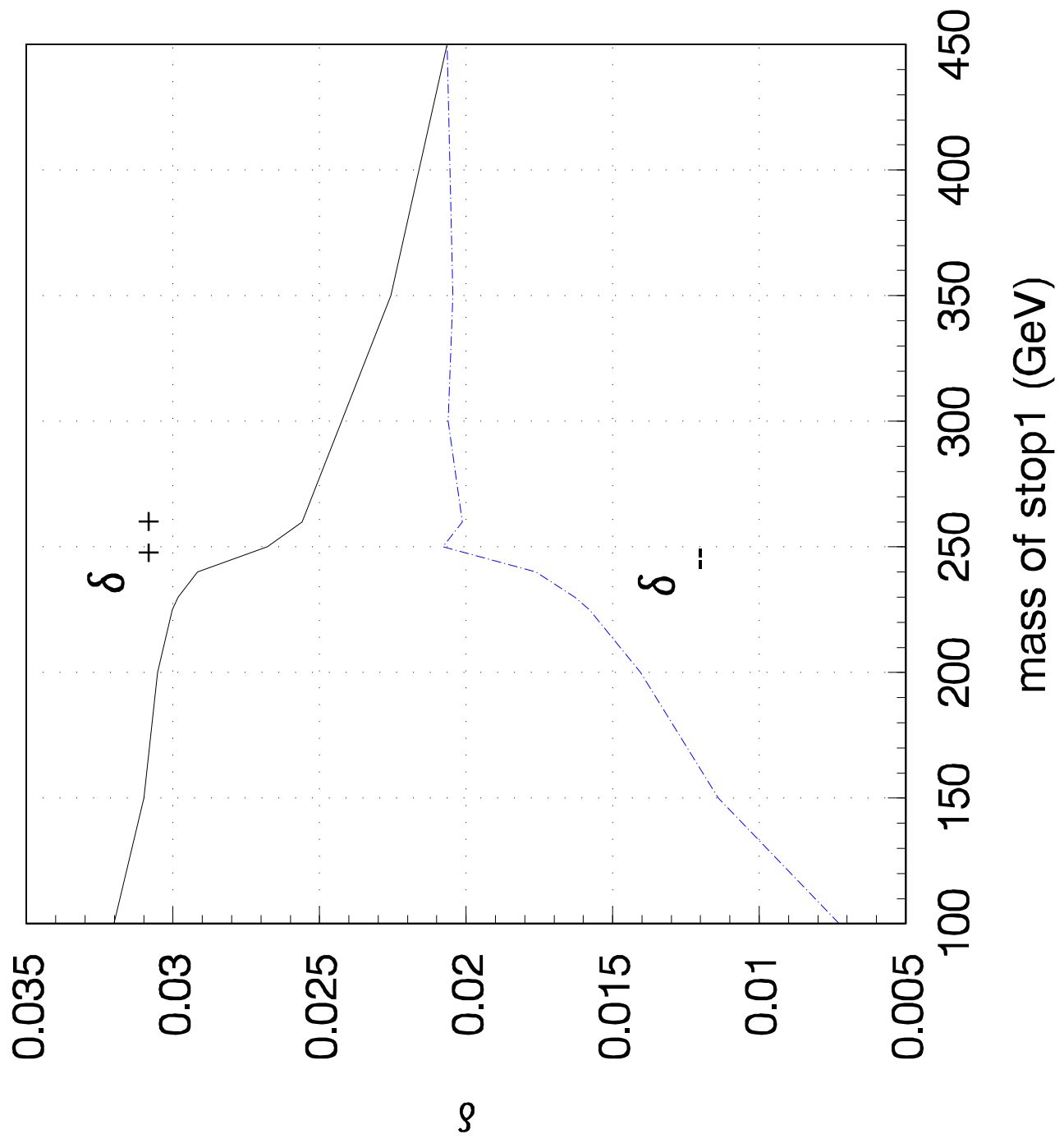


Fig.5 (b)

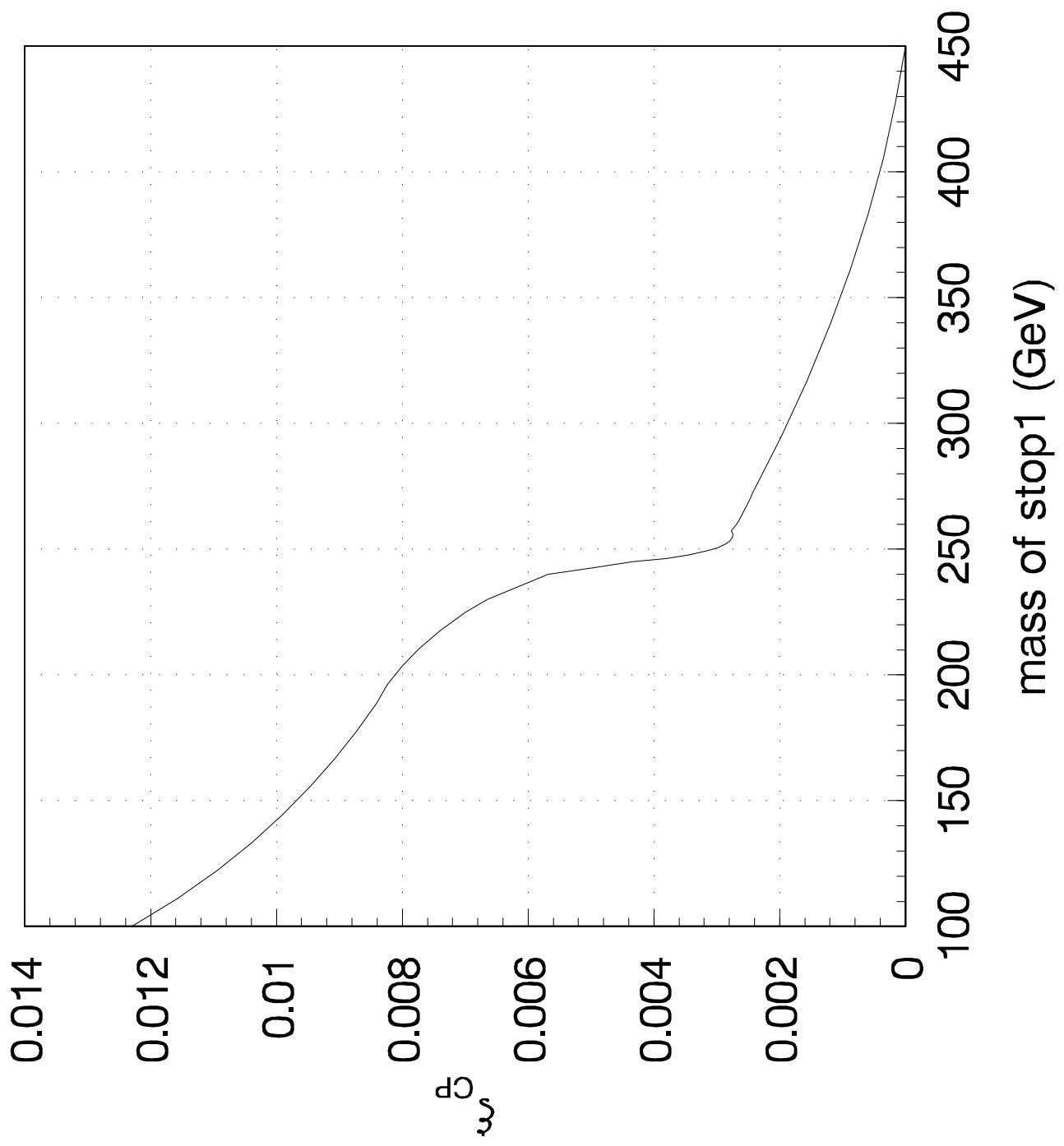


Fig.6 (a)

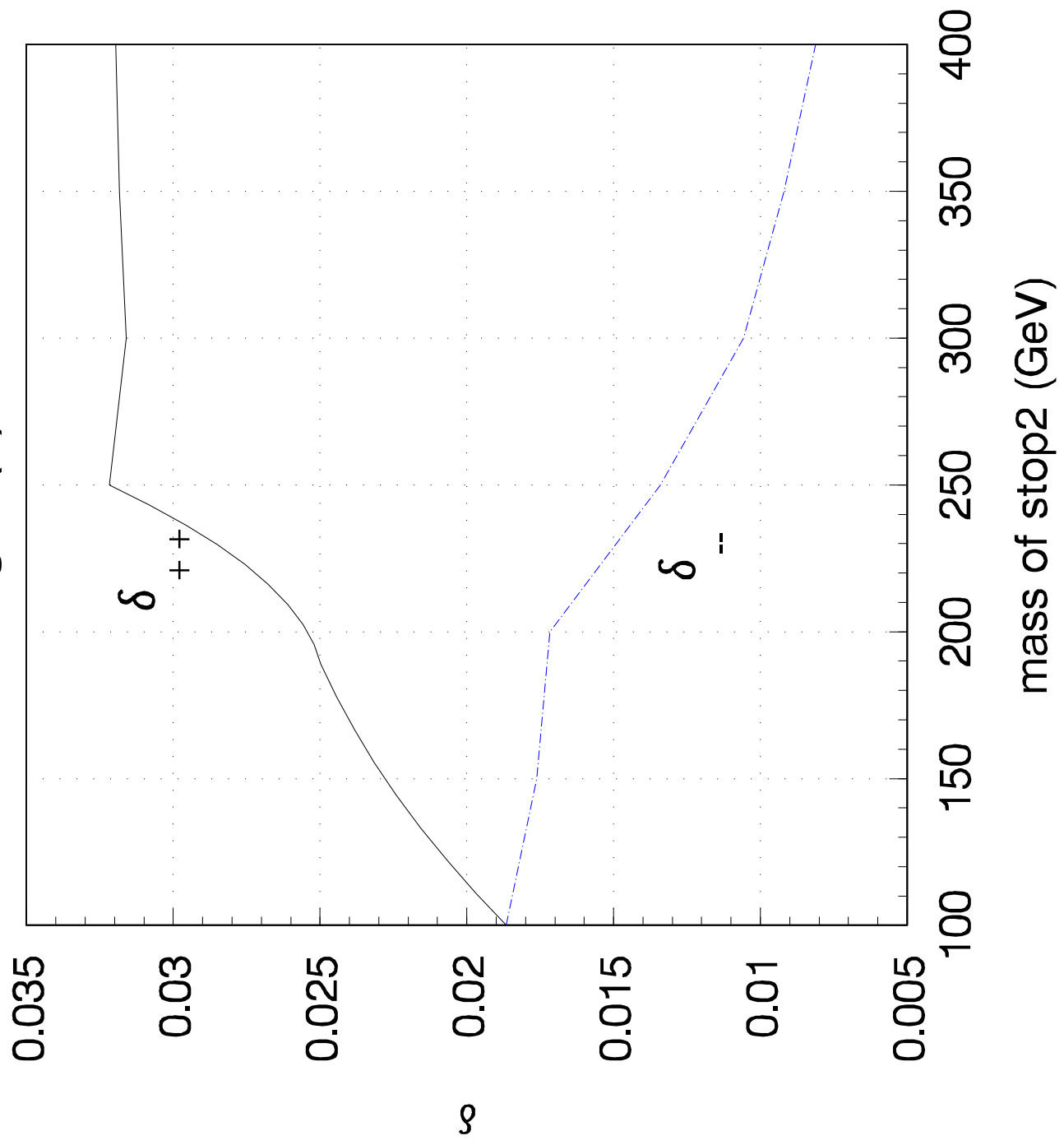


Fig.6 (b)

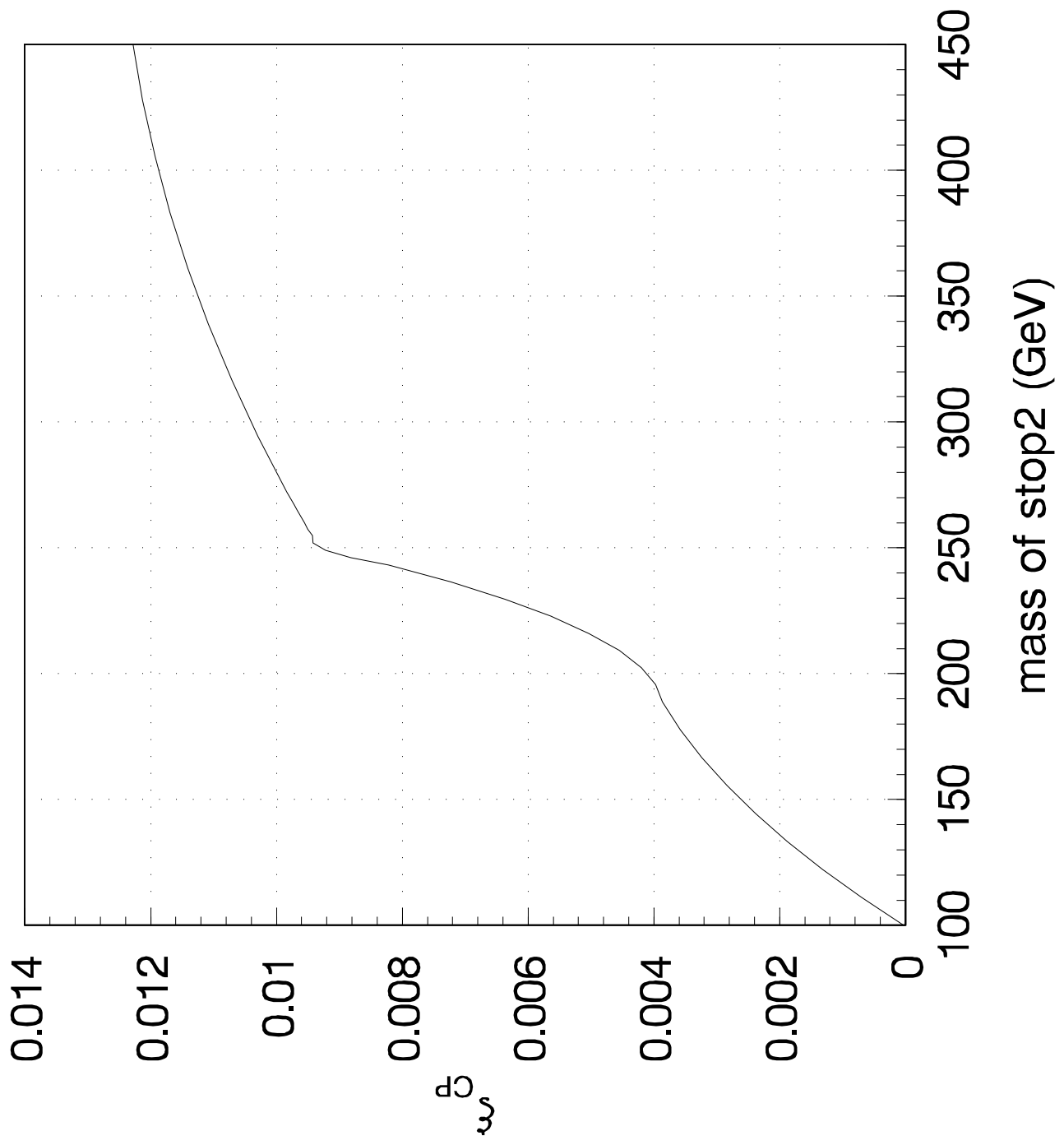


Fig. 7 (a)

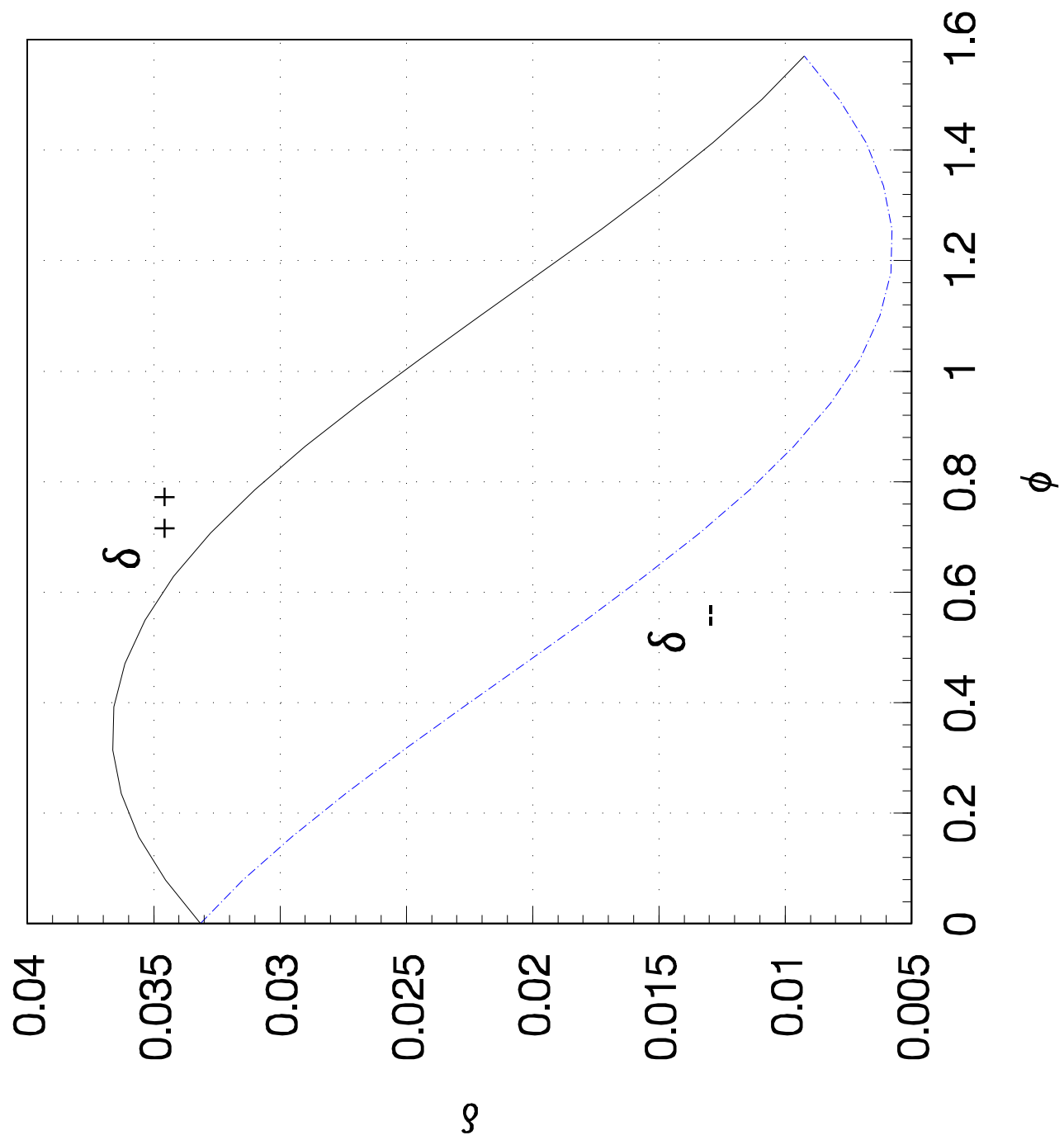


Fig.7 (b)

